High-Resolution NMR Spectroscopy of Sample Volumes from 1 nL to 10 µL

ARTICLE *in* CHEMICAL REVIEWS · OCTOBER 1999

Impact Factor: 46.57 · DOI: 10.1021/cr980140f

5 AUTHORS, INCLUDING:

Dean L. Olson
University of Illinois, Urbana-Champaign
34 PUBLICATIONS **1,275** CITATIONS
SEE PROFILE

Jonathan Sweedler
University of Illinois, Urbana-Champaign
510 PUBLICATIONS **15,003** CITATIONS
SEE PROFILE

High-Resolution NMR Spectroscopy of Sample Volumes from 1 nL to 10 μL

Michael E. Lacey,[†,§] Raju Subramanian,[‡,§] Dean L. Olson,[†,§,||] Andrew G. Webb,[‡,§] and Jonathan V. Sweedler*[,†,§]

Department of Chemistry, Department of Electrical and Computer Engineering, and the Beckman Institute, University of Illinois at Urbana–Champaign, Urbana, Illinois 61801

Received February 24, 1999 (Revised Manuscript Received July 30, 1999)

Contents

I. Introduction

Complete structural elucidation of an unknown compound, whether it is the product of a multistep synthesis, a potent extract from a natural source, or even a component of a waste stream, generally requires a battery of analytical techniques. Among common methods, infrared spectroscopy (IR), mass spectrometry (MS), and nuclear magnetic resonance (NMR) spectroscopy typically provide the most extensive chemical information. However, as shown in Table 1, NMR significantly trails these other techniques in terms of the minimum sample amount for an analysis. Nonetheless, NMR spectroscopy fulfills a critical role through its ability to produce unmatched structural information and also to provide data on both intermolecular and intramolecular dynamics. Applications of this technique range from determination of three-dimensional structures of large proteins[1] to the analysis of very small amounts of products from combinatorial syntheses.[2] Furthermore, NMR spectroscopy features an experimental versatility virtually unsurpassed in a nondestructive, analytical method. Although NMR data would prove extremely valuable in many important mass-limited situations, its poor mass sensitivity has, until recently, precluded its routine use in trace analysis.

To accommodate the particular research needs of an analyst, NMR methods vary in complexity from simple one-dimensional proton spectra to multinuclear, multidimensional data sets which typically take over 1 week to acquire. Considerable effort in the past two decades has centered on the development of pulse sequences to determine various physical, chemical, and dynamical properties of analytes. While a thorough background and theoretical treatment of NMR and its myriad experiments lies beyond the scope of this review, the interested reader is encouraged to explore this literature.[3−6]

Despite continuous improvements in the homogeneity and field strength of superconducting magnets during the last 15 years, currently available magnetic fields yield NMR transitions of very low energy. Since the transition energy is small with respect to kT at room temperature (where k is the Boltzmann constant), the population difference between the upper and lower energy states represents a minuscule fraction (typically $<0.01\%$) of the total number of molecules. Since the NMR signal depends on this difference in populations of the two energy states, it is a relatively insensitive detection method.

Many technical advances have been developed to increase the intrinsic NMR sensitivity. One approach utilizes higher magnetic field strengths since the NMR sensitivity increases as the $^7/_4$th power of the magnetic field strength.[7] High-resolution NMR spectrometers employ superconducting magnets which now reach field strengths as high as 21.1 T (a proton precession frequency of 900 MHz). However, this field strength represents the upper limit of current su-

|| Present address: Magnetic Resonance Microsensors Corp., 101 Tomaras Ave., Savoy, Illinois 61874.
† Department of Chemistry.
‡ Department of Electrical and Computer Engineering.
§ The Beckman Institute.

10.1021/cr980140f CCC: $35.00
Published on Web 00/00/0000 PAGE EST: 19.9

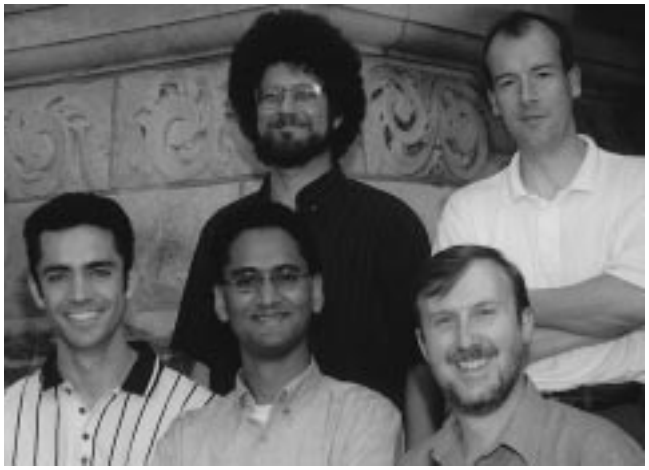

Michael E. Lacey (first row, left) received his B.S. degree in Chemistry from Texas A&M University in 1996. As an undergraduate, he conducted research with Professor Daniel Romo in the synthesis of marine natural products and with Professor Paul Lindahl in the investigation of inhibitor effects on the metalloenzyme *Clostridium thermoaceticum*. He is currently a senior graduate student at the University of Illinois at Urbana–Champaign, working with Professor Sweedler toward the development of nanoliter-volume NMR probes as detectors for capillary separations and static analyses of mass-limited samples. His research focuses on combining the high information content of NMR spectroscopy with microseparation methods such as capillary electrophoresis and capillary liquid chromatography for biologically relevant analyses.

Raju Subramanian (first row, middle) received his B.Sc. (Honors) degree in Chemistry from St. Stephen's College, Delhi University, India, in 1989 and his Ph.D. degree in Physical Chemistry from the State University of New York at Stony Brook in 1994. He spent 2 years as a postdoctoral researcher with Professors Gina Hoatson and Robert Vold characterizing guest motion in urea inclusion compounds by deuterium NMR. He joined Professors Webb and Sweedler as a postdoctoral research associate in 1996. His research focuses on the development of microcoil NMR for applications in the following three areas: (a) structure elucidation of mass-limited small organics, (b) hyphenation with microscale HPLC, and (c) extension to mass-limited proteins.

Dean L. Olson (first row, right) completed his Ph.D. degree in Analytical Chemistry from the University of Illinois in 1994. He then joined the academic research group of Professor Sweedler performing the first high-resolution and sensitivity studies with nanoliter-volume NMR microcoils. He also conducted the first experiments using high-resolution NMR as a detector for capillary electrophoresis. He is now employed at MRM Corp. (Savoy, IL) conducting research toward the commercial development and application of capillary-based NMR probes.

Andrew G. Webb (second row, right) received his Ph.D. degree in Medicinal Chemistry from the University of Cambridge in 1990 under Professor Laurie Hall. He was a postdoctoral researcher in the Department of Radiology at the University of Florida before joining the faculty in the Department of Electrical and Computer Engineering at the University of Illinois at Urbana–Champaign. He is currently an Associate Professor, with a full appointment in The Beckman Institute for Advanced Science and Technology. His research areas include the design of microcoils for NMR of mass-limited samples, the use of MRI temperature mapping for hyperthermia, and human brain mapping using functional MRI.

Jonathan V. Sweedler (second row, left) received his Ph.D. degree in Analytical Chemistry from the University of Arizona in 1989 under Professor M. Bonner Denton and then spent 3 years at Stanford with Professors Richard Zare and Richard Scheller developing new methods to study neurotransmitters in individual neurons. He is currently a Professor of Chemistry, Neuroscience, and of the Beckman Institute for Advanced Science and Technology at the University of Illinois. His current research interests are twofold: first, he is developing information-rich methods with improved mass sensitivity for nanoliter-volume samples, including microcoil NMR, mass spectrometric imaging, and capillary-scale separations. In addition, he applies these techniques to understanding the role of neurotransmitter and neuropeptide co-transmission and the regulation of behavior in well-defined neuronal networks of opisthobranch molluscs.

perconducting technology, and the next significant leap forward will require radically different designs and materials. A second, highly novel strategy utilizes polarization transfer from optically pumped nuclei (e.g., ^{129}Xe) via spin polarization induced nuclear Overhauser enhancement (SPINOE).[8−10] With this method of sensitivity improvement, signal enhancements of ∼50-fold for ^{1}H and greater than 70-fold for ^{13}C have been realized for soluble compounds in liquid xenon.[10] While the SPINOE technique is not limited to a particular NMR sample size regime, substantial sensitivity increases are not realized for all analytes. A third approach limits the receiver coil noise and increases the coil quality factor by using either high-temperature superconducting materials[11,12] or cryogenically cooled coils.[13,14] While this method improves the NMR sensitivity for all analytes, the large thermal gradient which must be maintained between the coil and liquid samples makes its application to the smallest radiofrequency (RF) coils difficult. By saturating electron spin systems which are coupled to nuclear spins, dynamic nuclear polarization (DNP) represents still another approach to increase the NMR signal intensity.[15,16] Flowing systems avoid several undesirable effects of static DNP analyses,[17] and examples of ^{13}C-DNP detectors for recycled-flow NMR and chromatographic separations have been reported.[18,19]

Table 1. Limits of Detection for Common Analytical Methods Used with Capillary Separations[38,120,121]

method	LOD (mol)
fluorescence	10^{-18}−10^{-23}
mass spectrometry	10^{-13}−10^{-21}
electrochemical	10^{-15}−10^{-19}
radiochemical	10^{-14}−10^{-19}
UV−vis absorbance	10^{-13}−10^{-16}
NMR	10^{-9}−10^{-11}

Although the magnet constitutes the most expensive part of a spectrometer, the overall system performance is usually dictated by the performance specifications of the NMR probe.[3] The probe consists of one or more RF coils which both excite transitions between energy levels via an oscillating magnetic field and also detect the weak signals produced by the precessing nuclei. NMR probe manufacturers offer a variety of designs and experimental capabilities which range in complexity from simple proton-detect probes to inverse triple resonance probes which feature RF coils designed for multiple nuclei, with circuits tuned to the proton, carbon, nitrogen, and deuterium precessional frequencies.

Recently, much commercial and academic research has focused on the optimization of RF coils for the analysis of trace materials. Significant increases in NMR sensitivity have been achieved through several different instrumental improvements. This article provides a comprehensive review of the application of NMR spectroscopy to nanoliter volumes for both static analyses and detection in capillary separations. Since no commercially available NMR probes currently have nanoliter-volume capabilities, we have also included descriptions of several high-sensitivity, high-resolution commercial probes which require sample volumes in the low tens of microliters. These microliter-volume probes represent the state of the art for commercially available NMR microprobes. First, we provide a brief overview of the major advances in NMR which have improved performance for mass-limited samples. Next, figures of merit

which aid in the comparison of NMR probes are presented. Additionally, a variety of NMR approaches to characterize microliter- to nanoliter-volume samples are described along with examples of both static homonuclear and heteronuclear experiments on mass-limited quantities. Finally, the coupling of capillary separation techniques with improved on-line NMR detection is examined.

II. Historical Perspective

The first detailed description of NMR spectroscopy using small, specialized RF coils for mass-limited samples was by Odelblad in 1966 who used continuous wave (CW) techniques to study the physical chemistry of mucus secreted from cells in the human cervix.[20] This study utilized a set of solenoidal microcoils with diameters from 200 to 1000 μm, with a fixed length of just over 1 mm. With these NMR probes in a high-strength permanent magnet (3.7 T), the proton chemical shift and spin−lattice (T_1) relaxation times of cervical secretions were measured. In 1979, Shoolery was the first to show high-resolution NMR spectra from a reduced-diameter RF coil.[21] Using RF coils which were designed for direct-observe ^{13}C NMR and closely fitted to the sample container in each case, a decrease in the diameter of the sample vial from 10 mm (1.5 mL volume) to 1.7 mm (15 μL) reduced data acquisition time by a factor of 40 for a given signal-to-noise (S/N) from a fixed sample mass of 5 mg of cholesterol. In this study, ^{13}C spectra were also obtained from as little as 1 mg in 16 h. For ^{1}H spectra, approximately the same data acquisition time was sufficient to detect 1 μg of cortisone acetate. Another application of solenoidal coils (2-mm diameter) in NMR spectroscopy allowed spectra to be acquired in under 3 min from the small superfused hind limb muscles of mice.[22]

Within the realm of magnetic resonance imaging, small diameter RF coils have also been used because of their enhanced sensitivity. As one example, microcoils (diameters as small as 1 mm) have been employed in conjunction with extremely high-strength gradient coils (~800 G/cm) to produce images from 100-μm slices of rat embryos with a 15-μm in-plane resolution.[23] Another approach to NMR microscopy utilizes an inductively coupled coil configuration in which a 1-mm solenoid (mounted directly beneath the sample) serves as the primary coil and a 2-mm solenoid acts as the secondary coil.[24] This arrangement allowed imaging of a single layer (40−70 μm thickness) of onion cells with a 4.5-μm in-plane resolution. Within the past several years, microcoils have even been used to acquire magnetic resonance images from single biological cells.[25−28] It should be noted that small RF coils have also been used extensively in electron paramagnetic resonance experiments.[29−31] For these applications, intrinsic line widths are several orders of magnitude greater than those for NMR spectroscopy, and so magnetic susceptibility effects can be largely ignored.

III. NMR Figures of Merit

In examining the extension of NMR techniques to mass-limited samples for both static analyses and on-line detection of capillary separations, several figures of merit are important to determine the feasibility of a particular experiment using a particular coil. For example, the structural characterization of a minuscule amount of a precious sample demands long acquisition times for a variety of experiments. On the other hand, the use of NMR as an on-line detector for separations places strict limits upon analyte observation time and thus the information content of the spectra. In the following two sections, figures of merit for NMR spectral resolution, mass and concentration sensitivity, and limits of detection are presented and evaluated for both static and flowing situations.

A. Spectral Resolution

Spectral resolution represents a very important figure of merit since it reflects the information content that can be extracted from an NMR experiment. Ideally, resonances should have Lorentzian shapes and narrow line widths (defined as the full width at half-maximum). To further characterize line shape, the width of the resonance signals at 0.55% and 0.11% of the maximum peak height are also often reported. The former is the height of the ^{13}C satellite peaks, and the latter represents 20% of this height. Since the height of a Lorentzian function is inversely proportional to its line width (LW), narrower resonance signals also result in higher sensitivity. For simple one-pulse experiments with liquid samples, factors such as thermal gradients[32] and the homogeneity of magnetic field in the sample region often limit the line width of the resonances in a spectrum. On the other hand, the digital resolution of the data set generally imposes the resolution limit for multidimensional experiments. For cases in which the digital resolution of the data has a significant impact on the apparent line width in the spectrum, resolution enhancement techniques such as zero-filling and linear prediction can be employed to improve the appearance of the spectrum.[33] In fabricating probes with more sensitive, reduced-diameter RF coils to examine smaller analyte amounts, the proximity of the probe materials to the sample becomes more detrimental to spectral resolution.[34−36] As a result, good line width specifications for small-volume probes pose a significant challenge. However, flowing systems can impose a limit upon spectral resolution which originates from short observation times rather than poor magnetic field homogeneity. Clearly, an acceptable LW for an NMR spectrum depends on the experimental conditions.

B. Signal-to-Noise, Sensitivity, and Limits of Detection

While the S/N of an individual peak in an NMR spectrum is usually defined as the height of the peak divided by the root-mean-square (RMS) noise, in the NMR literature the RMS noise is usually multiplied by 2 for reasons that can be attributed only to tradition. Several factors contribute to the signal strength, including the nuclear precession frequency, the RF receiver coil size and geometry, the sample

concentration and volume, the number of magnetically equivalent nuclei which give rise to a particular resonance, and the line width of the resonance. Furthermore, parameters such as the number of acquisitions (NA) and total acquisition time (t_{acq}) can significantly affect spectral results. As the noise in an NMR spectrum increases as $NA^{1/2}$ while the signal is directly proportional to NA (for a fully relaxed system), S/N varies with $NA^{1/2}$. Because NA is directly proportional to t_{acq}, S/N also increases as $t_{acq}^{1/2}$.

Of course, S/N in the frequency domain depends heavily upon the degree and type of data processing employed in the time domain. Throughout the history of FT-NMR spectroscopy, various mathematical operations (e.g., exponential, Lorentz-Gaussian, sine-bell, trapezoidal multiplication) have been developed which can enhance S/N at the expense of spectral resolution and vice-versa.[33] While NMR performance depends on acquisition and processing parameters for a particular sample and set of conditions, probe comparisons mandate specification of standard conditions for data collection and processing. However, many NMR spectroscopists and instrument manufacturers have developed measures of performance which are used only in NMR. In contrast, we prefer figures of merit which facilitate comparisons among NMR probes and evaluation of NMR with respect to other analytical methods.

At this point, a distinction should be made between the total sample volume required for an NMR analysis, V_{tot}, and the volume of sample observed by the RF coil, V_{obs}. The fraction V_{obs}/V_{tot} reflects the sample observation efficiency, and ideally this observe factor, f_o, should equal 1 ($V_{obs} = V_{tot}$). Because of magnetic susceptibility discontinuities at air and container interfaces, the sample usually extends beyond the coil region to provide quality data; in such cases, $V_{obs} < V_{tot}$. For instance, 5-mm tubes used for conventional NMR probes typically require 500−700 μL, only about 1/3 of which resides in the V_{obs} region of the NMR coil. Clearly, a limit of detection (LOD), defined in terms of the concentration or mass of sample which yields a S/N of 3, for the entire sampling system can be significant for analyte-limited applications. However, the signal from the sample within the RF coil will be used as the basis for comparisons of probe sensitivity in this paper. By focusing on V_{obs}, factors associated with sample loading are isolated and the fundamental limits of probe performance can be assessed more directly.

In general, NMR users are accustomed to an expression of S/N for a given analyte concentration. For example, the standard test for ^{1}H NMR sensitivity of high-field instruments consists of a single scan of 0.1% ethylbenzene in $CDCl_3$.[37] Although the results of this test are generally reported as the S/N, such a method is not appropriate for very small V_{obs}, where analyte amounts may be 5 orders of magnitude less than that for a 5-mm probe. In these cases, a number of acquisitions must be accumulated or the concentration must be increased to give a meaningful result. Consequently, this performance parameter can be more explicitly defined as time-normalized concentration sensitivity

$$S_c = \frac{\mathrm{S/N}}{\mathrm{C}\cdot t_{acq}^{1/2}} \quad (1)$$

where C is the sample concentration and $t_{acq}^{1/2}$ accounts for the total experiment time. Such a definition, however, may not accurately reflect the performance of a probe which has been designed for mass-limited samples. In such a case, a more appropriate indicator of probe performance is the mass sensitivity

$$S_m = \frac{\mathrm{S/N}}{\mathrm{mol}\cdot t_{acq}^{1/2}} \quad (2)$$

where the mole amount refers to the portion of the sample which resides within V_{obs}. The V_{obs} and sample concentration are used to compute the moles of observed sample. In contrast to S_c, S_m does not require designation of the tube diameter for a sensitivity test but instead incorporates the observe volume into the computation of sample amount. In both cases, the analyst can trade gains in S/N for reduced data acquisition time or sample quantity.

To emphasize the distinction between S/N and the intrinsically instrumental nature of sensitivity, suppose that NMR spectra are acquired and processed under identical conditions for 5- and 10-mm diameter cylindrical tubes in a fixed RF coil with the same analyte at equal concentrations. Because the number of spins in the 10-mm tube is 4-fold greater than in the 5-mm tube, the resultant signal magnitude, the corresponding S/N, and S_c exhibit a 4-fold increase. However, since S_m does not depend on the volume of sample examined,[3,38] utilization of S_m instead of S_c can yield more appropriate probe comparisons for mass-limited samples. In essence, the sensitivity of an NMR probe results from factors which include diameter, geometry, and quality factor of the RF coil, as well as other hardware specifications.

For a fixed coil size and line width, S_c is directly proportional to the fraction of volume within the coil which is occupied by sample. This parameter, called the coil filling factor, f_c, is readily computed from the inner diameter of the sample container and the NMR coil diameter (d_c). If the NMR coil is wound directly on the sample container, $f_c = (\mathrm{i.d./o.d.})^2$. These considerations establish both S_m and S_c as useful figures of merit in NMR probe evaluation.

An additional figure of merit to consider especially when comparing NMR probes for use as detectors in separations is the normalized limit of detection (nLOD). These values are affected by the experiment time as well so that

$$\mathrm{nLOD_c} = \frac{3Ct_{acq}^{1/2}}{\mathrm{S/N}} \quad (3)$$

and

$$\mathrm{nLOD_m} = \frac{3mol\cdot t_{acq}^{1/2}}{\mathrm{S/N}} \quad (4)$$

where the mole quantity again refers to that amount of sample in V_{obs} and the S/N corresponds to the peak of interest. The nLODs not only reflect probe sensitivity but also allow the user to compute the approximate mass or concentration of sample needed to acquire a desired S/N for a specific spectral peak using a particular probe and acquisition time.

Performance comparisons of NMR probes employed under different analytical situations are rendered more easily using the figures of merit described here. The relative importance of these figures of merit depends on the amount of sample available and the acceptable concentration range for a given experiment. These performance criteria are readily obtained and very useful in choosing a probe for a particular analysis. For instance, in the cases of many probes, only a fraction of the total sample lies within V_{obs}. A mass-limited condition generally calls for the greatest S_m, which is usually the probe with the smallest coil. A situation which is not mass-limited or where the sample already exists in a relatively large volume and cannot be concentrated benefits by using the probe with the largest S_c, which usually has the biggest V_{obs}.

IV. Approaches To Augment NMR Probe Performance

A. Microsample Tubes and Magnetic Susceptibility Plugs

The simplest approach to increasing the signal-to-noise of the NMR experiment, without having to redesign the RF coil, utilizes smaller sample tubes (which may even feature glass which is matched to the magnetic susceptibility of the solvent) or tube inserts to decrease the volume required for an experiment.[39] If the sample volume is reduced by a factor of 4, for example, the concentration can be correspondingly increased by a factor of 4, maintaining the same total number of spins. For analytes dissolved in conductive media, the decrease in V_{tot} can reduce the noise contribution from the sample and the S/N of the spectrum will increase. Alternatively, the sample can be contained in a spherical microcell. This places all of the sample within the active region of the RF coil and increases the observe factor to unity. The spherical shape of the cell is necessary to minimize the magnetic susceptibility induced line broadening that occurs since the sample/air and glass/air interfaces are now all contained within the coil. Such a strategy is straightforward and easily implemented, but the lower volume limit for commercial products is currently 18 μL.[40]

Another approach to small-volume NMR spectroscopy is to insert plastic plugs (matched to the susceptibility of the solvent) within a tube designed and optimized for larger volumes. These plugs are intended to restrict the sample to the active region of the RF coil, again increasing the observe factor so that it approaches unity.[40] For a 3-mm o.d. tube, for example, plugs allow a minimum sample volume of ~60 μL. No such susceptibility-matched inserts are commercially available for the nanoliter regime, although liquid perfluorocarbon susceptibility-matched plugs have recently been demonstrated for solenoidal microcoils with observe volumes less than 1 μL.[41] While these approaches increase the sample observation efficiency, the overall performance of the NMR probe can be further improved by making changes to the RF coil.

B. Reduction in Saddle-Type Coil Size

For the most part, the RF coils of standard high-resolution NMR probes are based upon a "saddle"-shaped geometry (see diagram in Figure 1A). From consideration of the spatial configuration of magnetic vector potentials, Hoult and Richards theoretically determined the sensitivity (as assessed by the RF field, B_1, per unit current, i) of this coil type as[7]

$$\frac{B_1}{i} = \frac{n\mu_0\sqrt{3}}{\pi}\left[\frac{2dh}{(d^2+h^2)^{3/2}} + \frac{2h}{d\sqrt{d^2+h^2}}\right] \qquad (5)$$

where n is the number of turns, μ_0 is the permeability of free space, d is the diameter of the coil, and h is its length. Clearly, reduction of the diameter and length of the coil increases sensitivity. In addition to the theoretical derivation of eq 5, Hoult and Richards also demonstrated that the length of the 90° pulse provides a direct measure of the sensitivity for a single RF coil system.[7] That is, shorter 90° pulse widths correspond to higher sensitivity RF coils. Virtually all commercial NMR probe manufacturers now offer probes which utilize the increased sensitivity of small saddle coils. The first significant development involved Varian's use of 1.7-mm tubes for both ^{1}H and ^{13}C NMR of mass-limited samples.[21,42−46] The introduction of an inverse-detection microprobe designed for 3-mm diameter tubes with total sample volumes of ~140 μL and observe volumes of ~60 μL added further capabilities to small-volume NMR.[47−51] By reducing the sample size to a 1.7-mm diameter tube, rapid data acquisition on reduced sample amounts was enabled for inverse-detection microprobes.[52−54]

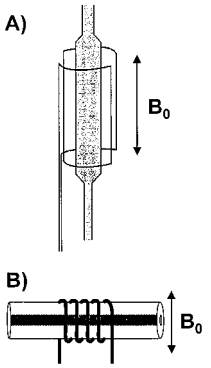

Figure 1. Examples of two RF coil geometries: (A) saddle type, (B) solenoid.

C. Solenoidal Coils and Magic Angle Spinning

For solenoidal RF coils (see Figure 1B), the sensitivity is given by[7]

$$\frac{B_1}{i} = \frac{\mu_0 n}{d\sqrt{1 + (h/d)^2}} \quad (6)$$

Therefore, assuming that the length-to-diameter ratio (h/d) is kept constant, the coil sensitivity will increase as the inverse of the diameter of the coil. For coils of diameters less than ~3 mm, the major noise source, even for lossy biological samples, arises from the resistance of the coil itself. Resistance depends on both the winding geometry (including wire diameter, number of turns, and turn spacing) and the resistivity of the conductor.

Varian introduced a series of probe designs termed "Nano·NMR probes" which use a 4-mm solenoidal RF coil which is oriented at the magic angle (54.7°) with respect to the static magnetic field (B_0). For a given length and diameter, the solenoidal design is approximately 2.5−3 times more sensitive than the saddle coil geometry described previously.[7] This design remedies the analyte wasted as a result of poor observe factors by placing the entire sample within the active region of the coil (i.e., $f_o = 1$). By spinning at the magic angle, the otherwise severe magnetic susceptibility effects are reduced and high-resolution spectra can be produced.[55] In contrast to conventional static NMR probes, rapid spinning of the sample at the magic angle also enables one to collect data from heterogeneous samples. To further improve the spectral quality, the coil is constructed using "zero-susceptibility" materials (as are most RF coils in high-resolution, high-sensitivity commercial probes). The maximum volume that can be accommodated is 40 μL, although good line shapes can be achieved for considerably lower volumes. For a spinning liquid sample, this probe obtains line widths that are only a few tenths of a Hertz greater than conventional high-resolution probes.

D. Microcoils

For solenoidal coils of diameter greater than about 100 μm, eq 6 can be expressed as the S/N per unit volume of sample

$$(S/N)_{puv} = \frac{{\omega_o}^2 [n/d_c\sqrt{1 + (h/d_c)^2}]}{\sqrt{n^2 d_c {\omega_0}^{1/2}/h}} \propto \frac{{\omega_o}^{7/4}}{d_c} \quad (7)$$

where ω_o is the nuclear precession frequency.[56] Since the mass sensitivity is dependent on the $(S/N)_{puv}$, the above expression demonstrates that S_m improves for a microcoil with a fixed length-to-diameter ratio as the coil diameter decreases (i.e., $S_m \propto 1/d_c$). Though the coil quality factor and inductance go down as d_c is reduced, a key performance parameter is the inductance per unit volume which increases as d_c decreases and produces the enhanced mass sensitivity of NMR microcoils.[56] Since thermal noise in the coil windings rather than sample noise is the primary contributor in microscopic studies, minimizing coil resistance also improves performance. For coils of diameter below 100 μm, the sensitivity dependence on the coil diameter is reduced to a square root relationship with the diameter. Since the 4-mm diameter solenoid used in the Varian probe is not limited by fabrication considerations, the sensitivity of the NMR experiment can be substantially improved by reducing the coil diameter. Figure 2 demonstrates the agreement between the theoretical and experimental increase in S/N per unit volume as the coil diameter decreases in size.[56]

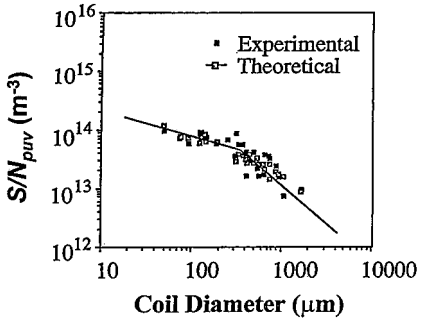

Figure 2. S/N per unit sample volume as a function of coil diameter. The $1/d$ and $(1/d)^{1/2}$ asymptotes do not account for the resistance of the leads and thus are not followed exactly by either theoretical or experimental data points. (Adapted with permission from ref 56. Copyright 1995 Academic Press, Inc.)

To date, NMR microcoils generally have been wound directly onto a capillary which functions as both sample container and coil form.[57,58] According to electromagnetic field theory, a sample enclosed by a perfectly uniform and infinitely long hollow cylinder (e.g., fused silica capillary) experiences a uniform static magnetic field.[59] However, the susceptibility variation in the materials near the sample (largely copper and its coating, adhesive, and air) can lead to localized distortions of the static magnetic field in the sample region. Furthermore, as the sample more closely approaches the coil windings, capillary coating, and surrounding environment, magnetic field inhomogeneities become more pronounced. The resultant line broadening decreases S/N and resolution. As a result, substantial attention has been devoted to studying the effects of coil proximity to the sample, especially considering the diminutive dimensions of microcoil NMR compared to traditional configurations.

While conventional microliter-scale probes use fabrication materials with near-zero magnetic susceptibility or sample plugs matched to the susceptibility of the solvent, the approach undertaken for microcoils surrounds the coil and capillary region with a fluid of magnetic susceptibility close to that of copper, the coil material. As shown in Figure 3, this has proved very effective in decreasing LW, improving line shape, and increasing S/N. Through the use of a susceptibility-matching fluid and a magic angle orientation of the solenoid relative to B_o, LW, line shape, and sensitivity can be improved significantly. This inexpensive and easily implemented strategy avoids problems associated with attempts to create materials of zero magnetic susceptibility for small dimensions.

To carry out complete structural elucidation (especially for complex molecules), the RF probe should have the capability of performing a variety of two-dimensional heteronuclear NMR techniques. In par-

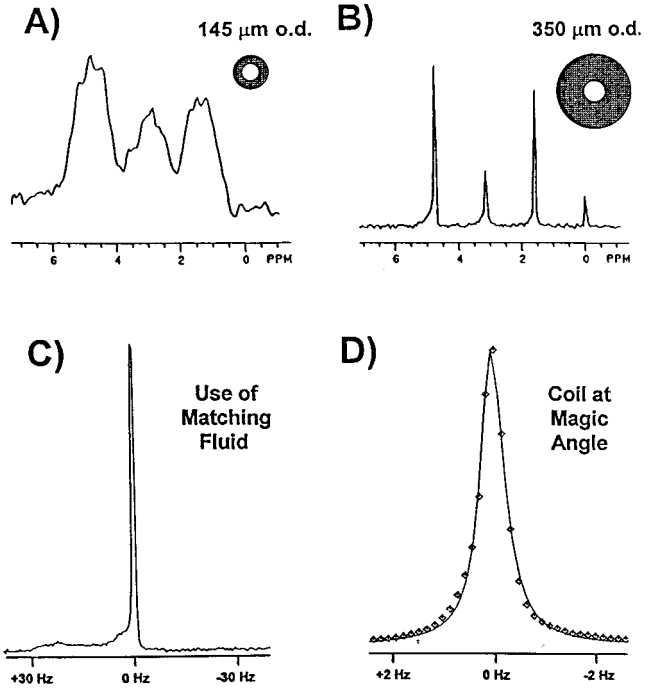

Figure 3. Progress in the improvement of line width and shape for NMR microcoils. (A) Without magnetic susceptibility matching fluid, line widths for arginine are 200 Hz for a thin-walled (75-μm i.d., 145-μm o.d.) capillary. (B) For a thicker-walled (75-μm i.d., 350-μm o.d.) capillary, without matching fluid, the line width is reduced to about 11 Hz but line shape is irregular.[79] (C) Effect of improved microcoil fabrication and the addition of magnetic susceptibility matching fluid to surround the microcoil for a spectrum of 10% H_2O/90% D_2O. Line width decreases to less than 1 Hz, S/N significantly improves, but line shape exhibits a baseline defect.[38] (D) Effect of a microcoil configured at the magic angle inside the magnet. Line width is 0.6 Hz for 10% H_2O/90% D_2O, and the data (◊) show no significant deviations in peak shape compared to the Lorentzian fit (—). All spectra obtained for protons at 300 MHz.

ticular, inverse-detection $^1H-^{15}N$ and $^1H-^{13}C$ experiments such as heteronuclear multiple quantum coherence (HMQC)[60,61] and heteronuclear single quantum coherence (HSQC)[62] find almost universal use in studies ranging from relatively simple structures with low molecular weights to more complex organic molecules. Although the microliter-scale probes described above feature both heteronuclear and homonuclear capabilities, no NMR probes are commercially available for the nanoliter-volume regime. As a result, we briefly include a description of the design considerations involved for multinuclear NMR microcoil probes.

Efficient double-tuned coils, ideally with a separate deuterium lock channel, are required for such experiments. For larger molecules such as proteins, considerably more sophisticated NMR pulse sequences such as HNCO[63,64] require the probe to operate at three or four separate frequencies. High efficiency is required of the proton observe channel. Ideally, the addition of circuitry allowing multiple tuning should not decrease the proton efficiency when compared to a single-tuned proton coil. In practice, some reduction must be accepted. Major design criteria for such inverse-detection probes include (a) minimization of losses of the multiple-tuned circuitry such that the heteronuclear channels are also as efficient as possible. High efficiency results in less power being deposited during decoupling, the decoupling bandwidth is maximized, and pulse widths are minimized. (b) isolation among the individual channels must be maximized: strategies include designs which yield geometric and/or electrical orthogonality and shielding using ground planes. Inverse-detection experiments involve proton detection while simultaneously using high-powered decoupling on the heteronuclear channel. Any cross-talk between the channels will lead to severe degradation of S/N.

The last criterion poses a particular challenge for microcoils since the lumped elements which comprise the multiple frequency impedance matching circuitries are typically positioned in much closer proximity than for traditional NMR probes. Electrical characterization of the probes includes the measurement of the S_{12} scattering parameter, defined as the reverse insertion voltage gain when source and load impedances are 50 Ω. That is, for 1 V applied to the inputs of the proton channel, S_{12} is a measure of the voltage detected at the output of the carbon channel if both channels have been impedance-matched to 50 Ω. For perfectly isolated channels, the scattering parameter will be 0. In reality, S_{12} values range from 0.1% (−30 dB) to 0.01% (−40 dB).

E. Microfabrication

Given the increased sensitivity which arises from miniaturized RF coils, microfabrication techniques can prove effective in establishing accurate geometries and good mechanical stability for smaller dimensions. As shown in Figure 4A, solenoidal microcoils have been fabricated by microcontact printing.[65] While high-resolution ^1H NMR spectra of ethylbenzene and acetone were demonstrated, the sensitivity of the printed microcoil was lower than others made by hand from copper wire. This decreased sensitivity was attributed to higher resistance which resulted from a lower cross-sectional area and higher resistivity of the electrodeposited copper compared to annealed copper. Planar coils with inner diameters less than 50 μm have been fabricated for aluminum and gold deposited on glass substrates. However, because of the potential for coupling dedicated preamplifiers and microcoils on a single substrate, gallium arsenide (GaAs) offers a more attractive RF coil material.[66,67] Planar receiver coils with 4.5 turns, a trace width of 3.5−10 μm, a trace separation of 3.5−10 μm, an i.d. of 97 μm, and an o.d. of 200 μm were fabricated. Through a combination of lift-off and electroplating technologies, the pattern was transferred from a mask written by conventional electron-beam lithography to a GaAs substrate. A 1.5-cm RF transmitter coil, constructed from a single turn of 18-gauge copper wire, was mounted orthogonally to the microfabricated receiver coil on the circuit board. Figure 4B shows a scanning electron micrograph of a planar microcoil.

For a simple model of n concentric turns and constant interturn spacing and trace width, the S/N per unit volume is

$$(S/N)_{puv} = \sum_n \frac{\dfrac{\mu_0}{D[1 + (2z/D)^{3/2}]}}{\sqrt{\sum_n \dfrac{4\rho D}{d^2}}} \quad (9)$$

where z refers to the on-axis distance from the coil, r corresponds to the resistivity, D is the o.d. of the spiral, and d is the diameter of the conductor.[57] According to this equation, the S/N varies slowly with coil diameter. While fewer turns require less space and fabrication effort, a greater number of turns yields increased inductance and a reduction in the capacitance required for impedance matching. Currently, the use of microfabrication techniques is in an inchoate stage. Although NMR spectra with line widths under 2 Hz have been achieved[57,65] and microfabricated fluidic systems have been coupled to chip-based NMR detectors,[68] magnetic susceptibility remains a significant issue. Additionally, planar microcoils must overcome the additional challenge of the extremely low signal strengths from subnanoliter observe volumes. Nevertheless, these techniques should prove essential as NMR spectroscopy examines continually smaller dimensions.

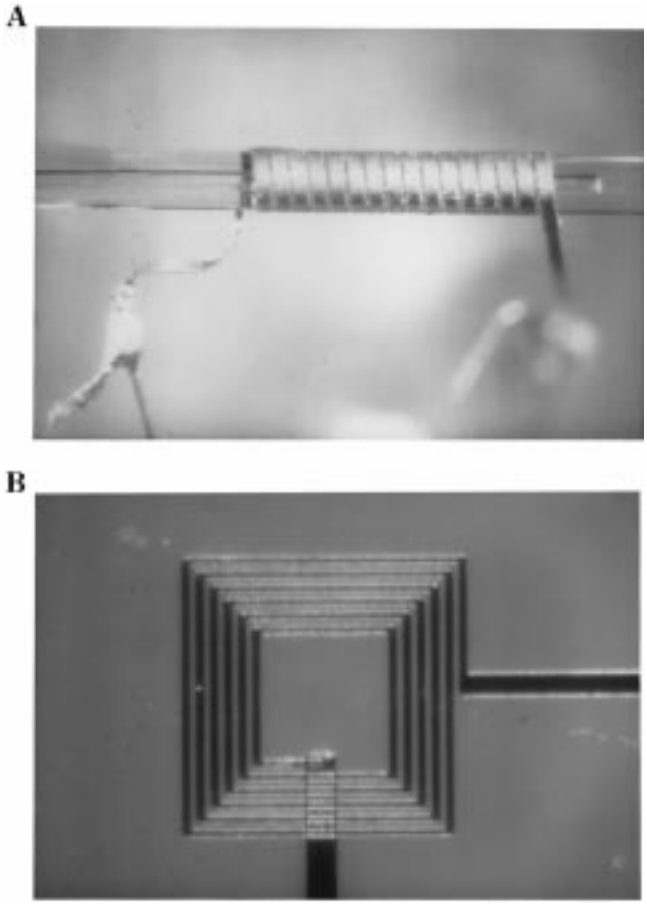

Figure 4. (A) Photograph of a 325-μm diameter solenoidal microcoil fabricated by microcontact printing. (Reproduced with permission from ref 65. Copyright 1997 American Institute of Physics.) (B) Scanning electron micrograph of a planar microcoil with an o.d. of 200 μm and an i.d. of 97 μm.

F. Direct Comparisons of Probe Sensitivity

An important question for an analyst is which NMR probe to use. We consider cases in which the sample is either mass-limited or concentration-limited but do not include planar microcoil probes in this comparison because their sensitivity is currently lower than the other small-volume probes. Since a valid comparison requires careful attention to sample preparation and NMR processing conditions for a particular analyte, a comprehensive survey of available commercial probes could not be garnered from the literature. The selected examples are provided to illustrate the general effects of RF coil design on mass and concentration sensitivity. In all cases, results were processed with a line broadening value equivalent to the line width of the resonance signals.

The first example derives from product literature for a probe designed for trace analysis. With a reduced-diameter saddle coil probe from Nalorac, a ^{1}H NMR spectrum was acquired from a total sample mass of 172 μg of sucrose in 23 μL of D_2O (21.8 mM sucrose) in a 1.7-mm o.d. sample tube. The single-scan S/N is 193 for the anomeric proton on a 600 MHz spectrometer with an acquisition time of 4.1 s. Since V_{obs} is approximately 60% of the total sample volume, the sensitivities (with appropriate units) are easily computed and appear in Table 2. Suppose an analyst wants to know what the result would be for the same sample mass in a 5-mm probe. A good comparison is to acquire a spectrum under identical NMR conditions with the same mass of sucrose (172 μg) dissolved in the observe volume of the 5-mm probe. On the basis of a coil length of 16 mm and a tube i.d. of 4.2 mm, V_{obs} = 222 μL (2.26 mM sucrose). The anomeric proton S/N is 136 for a single scan on a 600 MHz Varian INOVA spectrometer using a Varian 5-mm proton detection probe. For the same data acquisition and processing parameters as well as comparable line widths and shapes, the resultant sensitivities from the 5-mm Varian probe appear in Table 2. Clearly, the mass sensitivity is better for the Nalorac probe, but the concentration sensitivity is superior for the 5-mm Varian probe.

To illustrate more clearly the effects of design parameters on performance, two microcoil probes are also included in Table 2. Microcoil probe A is 1-mm long and is wound on a capillary with a 75-μm i.d./360-μm o.d. (V_{obs} of 5 nL);[38] microcoil probe B is 1.6-mm long and has a coil diameter of 850 μm and a V_{obs} of 620 nL. The performance indicators in Table

Table 2. Performance Comparisons of Several NMR Probes

figure of merit	Varian 5-mm	Nalorac SMIDG	microcoil probe A[a]	microcoil probe B[a]
S_c (S/N·mM^{-1}·s$^{-1/2}$)	30	4.4	0.028	0.95
S_m (S/N·μmol^{-1}·s$^{-1/2}$)	134	320	5580	1530
nLOD$_c$ (mM·s$^{1/2}$·S/N^{-1})	0.10	0.69	110	3.2
nLOD$_m$ (nmol·s$^{1/2}$·S/N^{-1})	22	9.6	0.54	2.0

[a] Data for microcoil probes A and B were collected at 300 and 500 MHz, respectively. These results were normalized to 600 MHz according to the relationship $[B_0]^{7/4}$.[7] Data for microcoil probe A from ref 38 was analyzed with respect to the signal from the anomeric proton. Data for microcoil probe B is courtesy of MRM Corp., Savoy, IL 61874.

2 show that the microcoil probe A achieves the highest S_m and requires the smallest sample size but is limited in S_c. The results for microcoil probe B confirm that a significant improvement in S_c and a proportionate decrease in LOD_c for the microcoil can be attained by increasing f_c.[69] Clearly, design parameters can be manipulated to suit particular experimental requirements.

In another example, a comparison was made for the same mass of material (400 ng of menthol) in the observed region of three NMR coils with $V_{obs} = 230$ μL (5 mm tube), 40 μL (Varian nanoprobe),[55] and 31 nL (microcoil; capillary 197 μm i.d., 340 μm o.d).[70] For the same mass of menthol dissolved in V_{obs}, the increase in mass sensitivity for the microcoil compared to the Varian microprobe allows acquisition of a comparable spectrum in 100-fold less time (9 min compared to 15 h).[70] Consequently, the S_m for the microcoil exhibits a 10-fold enhancement ($100^{1/2}$) compared to the Varian nanoprobe.

Consider a promising natural product of which only 100 pmol of material has been isolated. If the sample is dissolved in a V_{obs} of 5 nL, the sample concentration is 20 mM. In contrast, dissolution of the material in 230 μL (V_{obs} for a typical 5-mm spinning tube) yields a concentration of only 440 nM. Each NMR probe contains the same mass-limited amount of sample in its respective V_{obs} regions. In this case, the microcoil obtains a significantly higher S/N for a given t_{acq}.[38] A mass-limited condition generally calls for the greatest S_m, which is usually the probe with the smallest coil.

Alternatively, consider NMR binding studies of neuropeptide receptors which typically require low concentrations (μM) to determine the point at which strong interaction ceases. In this situation, one has to sacrifice S_m to gain overall S/N by using a larger-volume sample. A situation which is not mass-limited or where the sample already exists in a relatively large volume and cannot be concentrated benefits by using the probe with the largest S_c, which usually has the biggest V_{obs}. Clearly, no single probe fulfills all needs, and one must employ the right tool for a particular application. Considerations of probe sensitivity are weighed against the amount of sample available for analysis and the acceptable concentration range for the particular experiment. Although the use of small sample volumes can be limited by such factors as sample loading and solubility, the microcoil approach clearly offers impressive performance gains.[57,58] Given the superior mass sensitivity of microcoil probes, their advantages in mass-limited applications are obvious.

V. Microliter-Volume Static NMR Spectroscopy

A. Natural Product Extracts

In many cases, compounds obtained from natural sources have contributed to advances in medicine, materials, and many other areas. Since these compounds are typically isolated in small amounts, NMR probes with high mass sensitivity are required. As one example, the 3-mm Nalorac probe was used along with a variety of other analytical techniques to solve

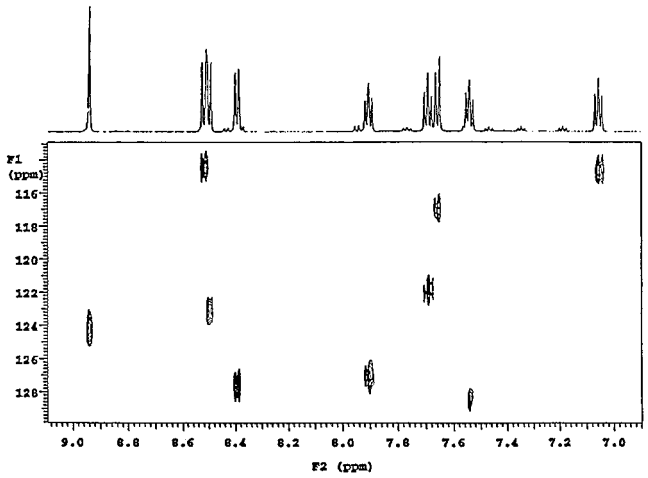

Figure 5. GHSQC spectrum of 550 nmol of cryptolepine dissolved in 25 μL of DMSO-d_6 acquired as 2048 × 16 hypercomplex files (2 × 16) with 16 transients per t_1 increment in a Nalorac inverse-detection probe. The data were acquired on a 600 MHz spectrometer in 12 min and processed to 1024 × 128 points by zero-filling the second frequency domain. (Reproduced with permission from ref 52. Copyright 1998 John Wiley & Sons, Ltd.)

the structure of cryptolepicarboline, a new indoloquinoline-β-carboline dimeric alkaloid isolated from *Cryptolepis sanguinolenta*, a shrub known for its medicinal properties.[51] For a total amount of sample of 250 nmol (100 μg), a one-dimensional ^{13}C spectrum required NMR data collection over the period of a weekend. In another application of this inverse-detection microprobe, HMQC experiments were performed on less than 100 nmol of a potent Caribbean ciguatoxin at 500 MHz.[52] With the standard 120 μL cell, total acquisition time for the HMQC spectrum was 231 h. The use of a Shigemi microcell reduced the volume to 67 μL and the total data acquisition time to 101 h. With a 1.7-mm Nalorac probe, 550 nmol of cryptolepine dissolved in 25 μL gave gradient-HSQC (GHSQC) and gradient-HMBC (GHMBC) in 12 min and 1.1 h, respectively.[50] Figure 5 shows the aromatic region of the GHSQC spectrum. In further analysis of the sample, an 8% impurity, corresponding to less than 50 nmol, was characterized from GHSQC and GHMBC spectra acquired in 25.5 and 56.5 h, respectively.[53] Long-range proton−nitrogen GHMBC spectra have also been obtained from a 1 mg sample (3 μmol) of the alkaloid strychnine dissolved in 30 μL of $CDCl_3$ in 18 h.[54] For weekend runs, sample requirements decrease to 1 μmol.

With regard to structural elucidation of unknown compounds, the Varian Nano·NMR probe has also proven useful in a variety of cases. As one example, the complete carbon skeleton of a novel steroid, 2-hydroxyandrosta-1,4-diene-3,16-dione, was determined using the $^{13}C-^{13}C$ INADEQUATE experiment with approximately 40 μmol of material: the total data acquisition time was 62 h.[71] In a second study, a novel glycosaminoglycan molecule was investigated.[72] Using a spin rate of 1850 Hz, TOCSY spectra were acquired in 30 h, DQF−COSY in 20 h, and ROESY in 60 h using 10 μg of material. Proteins and peptides have also been characterized with this technology. For instance, a study was conducted on

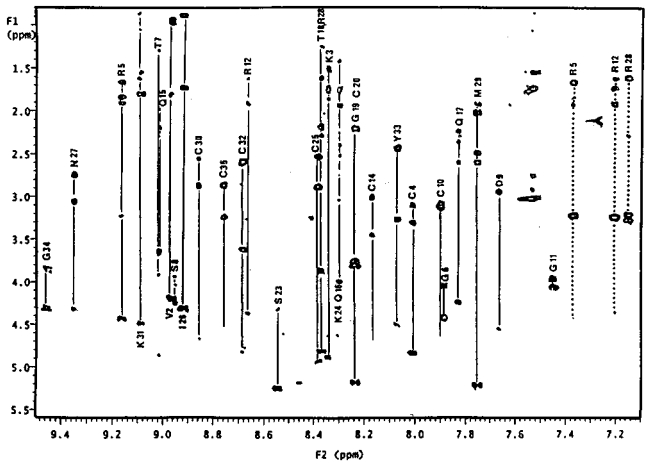

Figure 6. Contour plot of a TOCSY spectrum of Pi1 obtained at 35 °C. Spin systems are labeled by sequential residue position; a line connects the full spin system. (Reprinted with permission from ref 74. Copyright 1997 American Chemical Society.)

renatured lysozyme obtained from fully reduced lysozyme under folding/oxidation conditions.[73] One-dimensional spectra from only 6 μL, corresponding to 50 nmol, were obtained in 32 scans. Two-dimensional TOCSY spectra were acquired in 3−7 h. Finally, the Nano·NMR probe was used to obtain the full three-dimensional solution structure of a novel peptide, Pi1, purified from the venom of the scorpion *Pandinus imperator*.[74] In this case, a limited sample of 150 μg (50 nmol) precluded the use of standard NMR probe technology. Using 40 μL of sample at a concentration of 0.8−1 mM, a range of two-dimensional experiments provided the requisite information for complete structural characterization. Figure 6 shows a contour plot of a TOCSY spectrum of Pi1.

B. Analysis of Combinatorial Chemistry Products

Through the combination of magic angle spinning (MAS) and high-resolution probe fabrication, the Nano·NMR probe enables on-bead studies of products from solid-phase syntheses. The first application to combinatorial chemistry examined 1.5 mg (3 μmol) of a test compound bound to a Tentagel solid-phase-synthesis resin in DMSO-d_6.[75] By spinning the sample at several kilohertz, significant improvements in the spectral resolution are achieved.[75,76] In another report, MAS and spin−echo spectroscopy were used to follow the lithium aluminum hydride reduction of a resin-bound methyl benzoate to the corresponding benzyl alcohol.[77] Short T_2 signals from the polystyrene were efficiently suppressed by using the spin−echo sequence, and high-resolution proton spectra at 500 MHz using the Nano·NMR probe clearly showed the difference between the reactants and products. In a similar vein, Sarkar et al. used a combination of proton and heteronuclear techniques in identifying moieties while still bound to a solid-phase resin bead.[78] Proton spectra were obtained at 500 MHz from [3,5-dimethoxy-^{13}C] benzoic acid coupled to a single 100-μm diameter resin bead. The sample amount was estimated to be 800 pmol per bead. However, considerable interferences from the solvent, impurities, and a background from the polystyrene bead itself were evident. By using a one-dimensional HMQC sequence with a ^{13}C-labeled compound, the ^{13}C-filtered proton spectrum of the labeled compound showed signals only from the protons of the 3,5-dimethoxy-^{13}C moiety, with excellent suppression of the other protons. The total data acquisition time was approximately 3 h. A two-dimensional ^{1}H−^{13}C HMQC spectrum was also run, with an experiment time of 17.5 h. For these latter experiments the solenoidal coil of the probe was tuned to ^{13}C and an outer decoupler coil tuned to the proton frequency. Since this Nano·NMR probe is designed for ^{13}C direct detection, some loss of efficiency compared to inverse detection is expected.

VI. Nanoliter-Volume Static NMR Spectroscopy

While the examples above show the utility of NMR for static analyses in the microliter regime, downscaling experiments to nanoliter volumes presents additional challenges. While the early reports[79−81] of nanoliter-volume NMR spectroscopy illustrated the potential of submillimeter coils, the relatively broad line widths (7−11 Hz) were too great to resolve most scalar couplings. In the initial report of high-resolution ^{1}H NMR of nanoliter-volume samples, a 130-fold improvement in mass sensitivity (relative to a conventional probe) was demonstrated for a microcoil with a 5-nL observe volume.[38] Figure 7 shows a spectrum acquired from 3.3 nmol of α-bag cell peptide from the sea slug *Aplysia californica*; the LOD is 124 pmol for an acquisition time of 11.8 min.[38] While this initial work was performed at 300 MHz, further refinements of such microcoil probes have included experiments at higher fields and the incorporation of a lock channel.[82]

While the majority of microcoil work has focused on ^{1}H NMR, nanoliter-volume probes have been fabricated for both direct and inverse detection of ^{13}C.[83,84] Since the S/N of inverse-detection experiments is less than that of homonuclear proton experiments, typical sample volumes used are larger than those described earlier. With optimized coil geometries and volumes of between 700 nL and 1.2 μL, with concentrations of 30−100 mM, high-quality HMQC and HSQC spectra have been obtained in a few hours.[84]

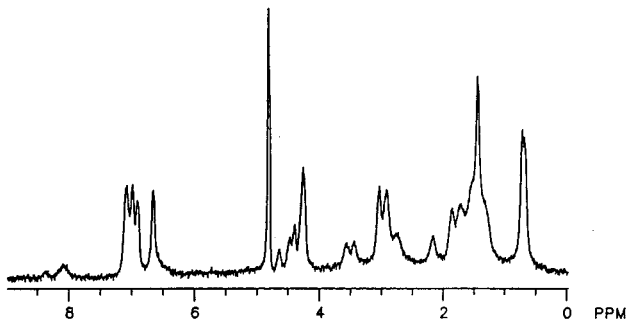

Figure 7. 300 MHz ^{1}H NMR spectrum of *Aplysia californica* α-bag cell peptide (residues 1−7). The 5-nL detection cell contains 3.0 μg (3.3 nmol) of peptide. The LOD is 112 ng (124 pmol) for an acquisition time of 11.8 min. (Reproduced with permission from ref 38. Copyright 1995 American Association for the Advancement of Science.)

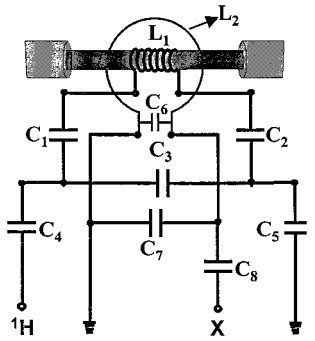

Figure 8. Representative circuit diagram for inverse-detection probes showing the requisite RF coils and capacitor layout.

Figure 8 depicts a circuit diagram of the inverse-detection probe used for either $^1H-\{^{15}N\}$ or $^1H-\{^{13}C\}$ experiments. The inner solenoidal coil is tuned to protons and the outer surface coil to the heteronucleus.[83] The surface coil consists of a single circular loop, 7 mm in diameter, and is mounted 1 mm from the microcoil edge. A chip capacitor is placed across the coil leads as close to the loop as possible. Although surface coils have a high sensitivity and are simple to construct, they are traditionally not used in high-resolution NMR due to a spatially inhomogeneous magnetic field profile. However, since the volume enclosed by microcoils is so small, the surface coils prove to be highly efficient both for pulsing and decoupling. Furthermore, the B_1 homogeneity is sufficiently high to produce a 180° pulse which inverts the magnetization cleanly during pulse-width calibration. The inductor and capacitor values used for proton operation at 500 MHz are shown in Table 3. The surface coil and solenoidal microcoil are housed in a plastic bottle which also contains the magnetic susceptibility matching fluid, as described previously. All the circuit elements, including the coils, are positioned on a 3 cm × 5 cm double-sided printed circuit board, with the impedance matching circuitry for protons and heteronuclear frequencies on opposite sides.

When impedance matched, the S_{11} parameters for ^1H and ^{13}C channels were each less than −30 dB, meaning that less than 0.1% of the power separately transmitted to each channel is reflected from the probe back through each individual channel. The S_{12} parameter, described earlier, was measured to be less than −25 dB at both frequencies. The typical ^1H and ^{13}C 90° pulse widths were 1.7 and 11.5 μs with 8 and 0 dB transmitter attenuations (amplifier rated outputs were 50 and 300 W, respectively). Full ^{13}C decoupling over a spectral width of 150 ppm was achieved using WALTZ-16 scheme with 14 dB decoupler transmitter attenuation. This probe has been used to measure $^1H-^{13}C$ correlations on several low molecular weight organic compounds.[83,84] As one example, Figure 9 shows a two-dimensional HMQC of chloroquine diphosphate in D_2O.

Table 3. Values of Circuit Elements Used in Inverse-Detection Probes

	^1H (500 MHz)	^{13}C (125.7 MHz)	^{15}N (50.7 MHz)
L_1	42 nH		
L_2		14 nH	14 nH
C_1	5.6 pF		
C_2	5.6 pF		
C_3	3.2 pF		
C_4	6.5 pF		
C_5	3.8 pF		
C_6		100 pF	100 pF
C_7		10.2 pF	330 pF
C_8		11 pF	20 pF

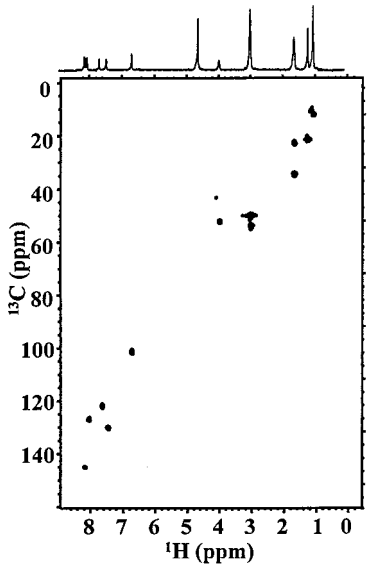

Figure 9. ^{13}C-decoupled HMQC spectrum of 54 mM chloroquine diphosphate in D_2O acquired with an inverse-detection microcoil probe. The 745-nL V_{obs} contains 40 nmol (13 μg) of chloroquine. The data, 32 transients per slice, 1024 × 128 (×2, hypercomplex) points, are acquired in 3.6 h. The data were zero-filled to 256 points in the ^{13}C dimension. A 40° shifted sinebell function was applied followed by Gaussian multiplication prior to Fourier transformation.

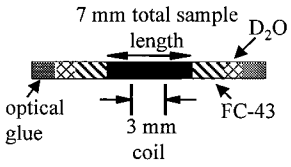

Figure 10. Example of liquid susceptibility matching plugs used with microcoils for limited-volume samples.[41]

Inverse-detection experiments can also be performed on a sealed capillary sample with careful preparation, with the setup in Figure 10. The liquid susceptibility-matching approach[41] described earlier allows observe factors of up to 70% without broadening the line width.[83,84] A sample plug is sealed in the center of a 3-cm long 700-μm i.d./850-μm o.d. polyimide-coated fused silica capillary. A 3-mm long solenoidal microcoil (consisting of 11 turns of 50 μm × 225 μm polyimide-coated copper wire) encloses the restricted sample and has a V_{obs} of 1.2 μL. The restricted sample has perfluorocarbon (FC-43) fluid plugs at either end of the sample. Short plugs of D_2O help prevent the formation of bubbles in the perfluorocarbon liquid. Figure 11 shows a two-dimensional HMQC spectrum of progesterone acquired using a fixed sample length of 7 mm. The unique inverse-detection microcoil probes described in this section make acquisition of two-dimensional $^1H-^{13}C$ correlation spectra possible for samples with masses as low

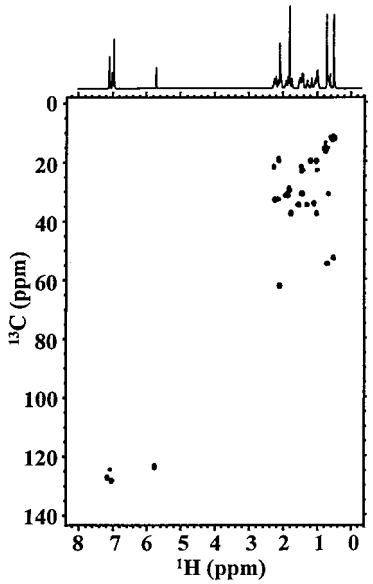

Figure 11. ^{13}C-decoupled HMQC spectrum of 31 mM progesterone in toluene-d_8 acquired with with the limited-volume configuration featured in Figure 10. A total sample amount of 85 nmol (27 μg) is used, with 37 nmol (11.4 μg) within the V_{obs}. The data, 48 transients per slice, 1024 × 128 (×2, hypercomplex) points, are acquired in 5.7 h. Processing as in Figure 9.

as tens of micrograms with data acquisition times of a few hours. This represents an order of magnitude improvement compared to the commercial microliter-scale NMR probes described earlier.

VII. NMR Detection of Capillary Separations

As practitioners of the chemical sciences continue to blur disciplinary boundaries through investigations of truly complex systems, analytical methods must correspondingly increase in their degree of sophistication. During the past two decades, hyphenated analytical techniques have become rather commonplace. Multimode separation and detection strategies are requisite in such diverse areas as characterization of pharmaceutical candidates, understanding chemical communication within living organisms, and geochemical analysis of planetary samples. In particular, NMR has been coupled to separation methods such as gas chromatography (GC),[85] supercritical fluid chromatography (SFC),[86] and gel-permeation chromatography (GPC)[85] as well as liquid chromatography (HPLC),[85,87] capillary electrophoresis (CE),[58,79,80,88−92] and capillary electrochromatography (CEC).[88−90,92] Some of the primary advantages of on-line (versus off-line) NMR detection in flowing systems include improved chromatographic resolution, consistent detector response, on-line data analysis, and faster data acquisition. Capillary separations offer the additional benefit of reduced solvent consumption. The experimental versatility of NMR spectroscopy as a detector for separations has been applied successfully to solve a wide variety of problems. However, this review focuses on the combination of NMR and capillary-scale (i.d. of less than 1 mm) separations. While the recent advances in NMR microprobe development outlined above have enabled NMR detection of microseparations, many of the capabilities of conventional NMR have not yet been applied to the capillary scale. The interested reader is encouraged to explore the literature for reviews of NMR coupled to conventional-scale separations.[85,87,93,94]

The joining of capillary electroseparation methods and capillary HPLC with NMR detection provides information complementary to existing methods. While Table 1 illustrates that LODs for CE with microcoil NMR detection are currently poorer than other on-line detection techniques, the ability to identify compounds on the basis of their NMR spectra and to spectrally discriminate among unknown peaks using multidimensional data merits exploration. Moreover, improvements in LODs will continue to accrue through further hardware developments. In contrast to conventional NMR probes, the enhanced mass sensitivity of reduced-diameter RF transceivers enables the coupling of one of the most structurally-rich detection schemes and highly efficient capillary separations.

A. Flow Effects

In designing NMR detection strategies for flowing separation systems, the effects of solution flow on the NMR line shape, S/N, and LW must be considered. In contrast to stopped-flow conditions which allow longer NMR acquisition times, the continuous flow associated with typical column separations imposes certain restrictions on NMR data. Flow of analyte through the detection coil reduces the effective longitudinal relaxation time of the sample by replacing pulsed spins with unpulsed spins, thereby allowing more rapid pulse repetition and improved S/N per unit time. In 1984, Laude and Wilkins reported a systematic study of the effects of flow rates on both NMR sensitivity and resolution for analytical-scale HPLC−NMR.[95] Wu et al. developed a model for microcoils and compared the S/N obtained with optimized pulse repetition rates as a function of coil diameter.[81]

In a similar fashion, the effective transverse relaxation time ($T_{2,Flow}$) may also be shortened. The decrease in $T_{2,Flow}$ due to the limited spin residence time (τ) may increase signal LW for any given spin not observed for a period long enough to allow full signal decay of the analyte within the observe volume of the NMR probe. In these cases, the effective transverse relaxation time of the analyte decreases in a flowing system and the signal decays more rapidly than for a static analysis. The resulting increase in line width due to flow is inversely proportional to τ.[95,96] Consequently, while higher flow rates allow faster pulse repetition and a possible increase in S/N, the degradation in LW may conceal important spectral information. As a result, the optimum flow rate for on-line NMR detection is a compromise among S/N, LW, and chromatographic resolution.[85]

In addition to the effects of flow on spectral resolution and data acquisition strategies, NMR possesses the capability of in situ flow characterization during a separation. Although not yet demonstrated on the capillary scale, pulsed field gradient (PFG) NMR techniques have been used to study

dispersion in packed HPLC columns.[97] From the average values of the axial and transverse apparent diffusion coefficients in a packed column over a certain volume of the bed, Tallarek et al. related the local value of the height equivalent to a theoretical plate of a chromatographic column to the velocity of the liquid. Furthermore, excellent agreement between theoretical studies of the plate height equation and the PFG−NMR results were demonstrated. Given this initial demonstration, the use of gradient NMR techniques for the in situ analysis of capillary separations holds great promise.

B. HPLC–NMR

Though demonstration of both stopped-flow and continuous-flow HPLC−NMR first appeared in the late 1970s,[98,99] this hyphenated technique has only recently begun to experience widespread use.[85] The development of suitable flow cells and techniques to optimize NMR acquisition conditions have laid the foundation for today's commercial HPLC−NMR instruments.[100−105] Sensitivity enhancements through higher-field magnets,[106,107] smaller-diameter transceiver coils, and increased dynamic range of receivers, combined with the availability of versatile solvent suppression techniques,[108,109] have also alleviated many of the initial problems of HPLC−NMR. Nonetheless, the relatively poor mass sensitivity of conventional NMR detection schemes, compounded by limited observation time for each analyte, has remained the primary challenge to on-line NMR detection of nanoliter volumes.

HPLC column eluent clearly represents a mass-limited condition. Typical HPLC−NMR detection cells have RF coil observe volumes in the range of 60−250 μL and are used in conjunction with conventional 2−4.6-mm i.d. columns. NMR probes designed for small amounts of material are well-suited to microbore and capillary HPLC because the higher efficiency separations result in higher sample concentrations eluting from the column. Typically, the analyte concentration in the peak maximum is inversely proportional to the square of the column i.d. Thus, the smaller the column i.d., the less a given sample is diluted prior to detection. As an example, Table 4 shows typical peak volumes and expected analyte peak concentrations for a 1 nmol injection. Note how capillary HPLC increases the analyte concentration more than 2 orders of magnitude, so that the combination of smaller and more efficient NMR probes coupled with smaller HPLC columns may represent a superior HPLC−NMR configuration. The improved S_m of reduced-diameter transceivers yields lower mass LODs and allows coupling of NMR to the more efficient microbore and capillary HPLC columns. However, downscaling HPLC−NMR 3 orders of magnitude to nanoliter regimes introduces several unique considerations.

Table 4. Typical Column Separation Parameters and Resultant Peak Concentrations for 1 nmol of Analyte

column i.d. (mm) and mode	flow rate (μL/min)	peak volume (μL)	Peak concentration (mM)
4.6 (standard)	1000	200	0.005
1 (microbore)	30	10	0.1
0.32 (capillary)	3	1	1
0.18 (capillary)	1	0.3	3

Conventional HPLC−NMR employs separation columns which are connected to NMR detection cells via open tubular capillaries with internal diameters substantially smaller than the column to avoid extracolumn band broadening. Since the band broadening introduced by the connections and transfer lines causes significant peak dispersion in capillary separations, on-column detection for small-volume HPLC is desirable. One technique[81] employs a solenoidal transceiver coil wrapped directly around the separation column. Attachment of the coil to the flow cell itself creates a detector with a high f_c, thereby improving concentration sensitivity. Such a design positions the detection cell perpendicular to B_o and takes advantage of the augmented sensitivity of solenoidal geometry.[7] An alternative approach utilizes saddle-type coils produced by Bruker with parallel alignment of the separation column with respect to the magnetic field.[88,110−112] With this arrangement, HPLC columns are inserted into the magnet so column types and diameters can be changed without altering the size of the transceiver coil. This experimental configuration allows effective shimming and permits column changes to occur without noticeable perturbation of magnetic field homogeneity. In both cases, to avoid negative effects of the HPLC apparatus on the magnetic field and vice versa, the pump and the solvent reservoir remain more than 1 m from the magnet. To maximize signal intensity, prepolarization of the nuclei through residence in the magnetic field for greater than 5 T_1 intervals establishes a Boltzmann distribution of nuclear spins.

The relatively large volumes and flow rates used with conventional (4.6-mm i.d.) analytical HPLC columns make the deuterated solvents conventionally used for NMR spectroscopy a significant part of the total experiment cost (except D_2O). Although halocarbons can eliminate ^{1}H NMR background signals, these solvents are not amenable to the majority of separations. To minimize the interference of solvent peaks, one can employ either solvent suppression techniques or deuterated solvents and smaller-diameter chromatographic columns to minimize solvent consumption. For continuous-flow experiments, solvent presaturation is not very effective because a fraction of the spins is constantly replaced in the V_{obs} region by unsaturated spins. The change in resonance frequencies for signals which accompany gradient elution poses an additional challenge. Despite considerable improvements in these methods,[109] solvent suppression usually renders spectral regions near the solvent signals unobservable. In contrast, the small volume requirements of microbore and capillary HPLC columns not only permit the use of gradient elution with completely deuterated solvents but also fulfill the desire for higher separation efficiencies and reduction of solvent consumption.

The first microbore HPLC−NMR experimental results were published in 1995.[81] In this initial report, a solenoidal microcoil was wrapped directly

around a fused silica capillary (250 μm i.d.; 360 μm o.d.) to create a V_{obs} of 50 nL and an f_c of 48%. For a separation of three amino acids and two peptides, submicrogram LODs were obtained on a 300 MHz spectrometer. However, this system represented a 100-fold mismatch between the estimated analyte peak volume of ~5 μL and the 50-nL observe volume of the detector, a condition far from ideal. The use of fast pulse repetition rates partially compensated for this problem (by taking advantage of new spins brought in by flow).

In another report of capillary HPLC−NMR coupling,[111] a 180-μm i.d. packed capillary was inserted within a 2.0-mm NMR probe to create a V_{obs} of 200 nL (f_c = 0.9%). For stopped-flow NMR data acquisition, the spectral resolution obtainable with this arrangement was ~1.5 Hz. This system was applied to the characterization of vitamin A derivatives, which tend to decompose or isomerize with exposure to air or light. A contour plot of the capillary HPLC−NMR chromatogram illustrated the ^{1}H NMR spectral differences between vitamin A acetate and its reaction products. However, no LODs or information about separation efficiency were included in this report.

Continuous- and stopped-flow NMR coupled to gradient capillary HPLC was first reported in 1996.[110] In this report, a 315-μm i.d. capillary was packed with reversed-phase particles before the NMR detection window to separate a mixture of dansylated amino acids. Mounted vertically within a ^{1}H/^{13}C 2.5-mm inverse-detection Bruker microprobe, V_{obs} for the capillary was 900 nL. Gradient elution yields a more efficient separation and offers a convenient means of sample preconcentration. The use of highly efficient capillary HPLC and a higher magnetic field strength (600 MHz) also provided improved performance. Though the capillary and NMR coil arrangement was not optimal (f_c = 1.6%), LODs of about 70 pmol were obtained under stopped-flow conditions for t_{acq} = 20 min.

Elucidation of the structure of a previously unknown kitol isomer (natural retinol dimer) represents a practical application of capillary HPLC with nanoliter-volume NMR detection.[112] Despite a decrease in the NMR coil diameter from 2.5 to 2.0 mm compared to their previous study,[110] f_c decreased to 0.8%. With a V_{obs} of 200 nL, the LOD was 150 pmol for a model compound in 7.7 min. Figure 12 illustrates the use of fully deuterated solvents for acquisition of spectra unhindered by solvent suppression. As shown in Figure 12A, the one-dimensional spectral data combined with the two-dimensional TOCSY experiment in Figure 12B allow unambiguous structural determination. Spectra were recorded when the chromatographic peak maximum had entered V_{obs}, as signaled by continuous monitoring of the ^{1}H NMR signal.

Another approach to joining capillary HPLC and NMR utilizes a fixed capillary NMR detection cell and allows fascile coupling to a variety of microseparation methods.[88] By treating a 60-μm i.d. fused silica capillary with HF and localized heat, Pusecker et al. increased the i.d. to 190 μm for a specific region of the capillary. In this report, the 240-nL detection cell

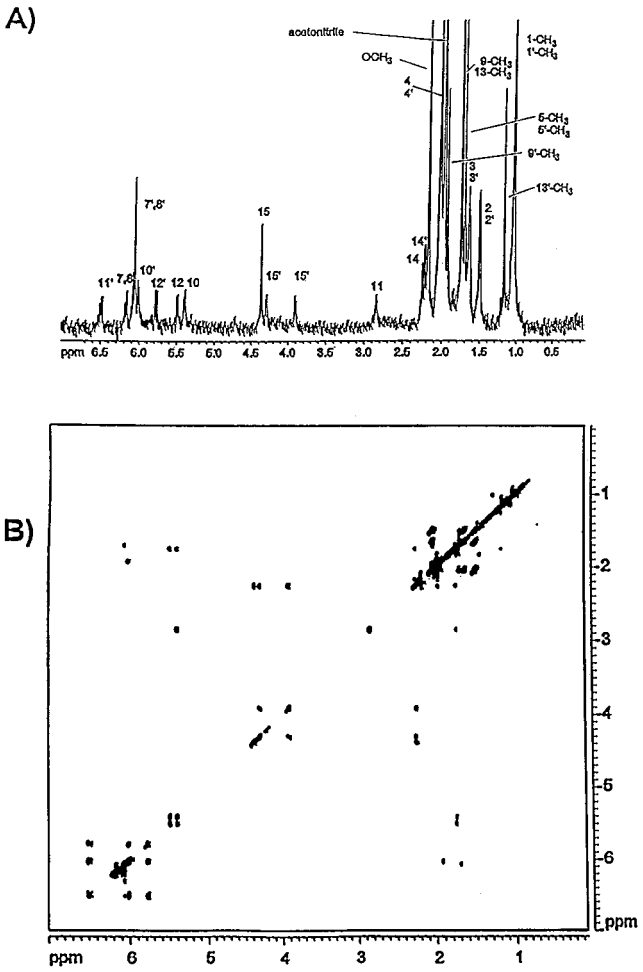

Figure 12. (A) Stopped-flow, capillary HPLC−^{1}H NMR spectrum including peak assignments of a kitol (natural retinol dimer) from a mixture of isomers. Capillary i.d., 180 μm; detection volume, 200 nL; data acquisition time, 5.3 min. (B) Phase-sensitive TOCSY of the same kitol. Total data acquisition time, 15 h. In both cases, the total sample mass injected onto the HPLC column is about 50 μg. (Adapted with permission from ref 112. Copyright 1997 American Chemical Society.)

was placed within a 2-mm Bruker microprobe and connected to a packed HPLC capillary via Teflon tubing. Such a configuration yields an f_c of 0.9% and line widths on the order of 2.5 Hz, after shimming on a chloroform signal for the hump test (3% chloroform in 97% acetone-d_6). In addition to increasing analyte observation times (for a flowing system), the enlarged detection cell facilitates shimming through a more stable lock and better S/N for the hump test. Capillary HPLC−NMR was demonstrated with this arrangement for both a mixture of alkyl benzoates and a 20% solution of hop bitter acids. Stopped-flow ^{1}H−^{1}H COSY data were presented for two of the hop bitter acids (t_{acq} = 13 h). Unfortunately, information about LODs was not included. These separations were performed in completely deuterated solvents and, as such, prevented solvent signals from overlapping with analyte signals in the NMR spectrum. Given the wide applicability of HPLC, many more examples of capillary HPLC−NMR will certainly appear in the coming years.

C. SFC–NMR

Though the union of supercritical fluid chromatography and supercritical fluid extraction with ^{1}H NMR has been reported,[113−117] this combination has never been demonstrated on the nanoliter scale. SFC−NMR employing CO_2 or various other supercritical solvents without a ^{1}H NMR background signal as the mobile phase eliminates the need for solvent suppression. Capillaries can withstand the elevated temperatures and pressures associated with supercritical fluids. Additionally, their diminutive volumes allow the economical use of deuterated organic polar modifiers. For these reasons, nanoliter SFC−NMR may appear soon.

D. CE–NMR

As a collection of efficient and flexible separation methods, capillary electrophoretic techniques have found widespread application in the analysis of charged and neutral species.[118,119] In contrast to HPLC where column dimensions can be manipulated over a substantial range, the i.d. of electrophoresis capillaries is generally restricted to less than about 100 μm to avoid problems from dissipation of Joule heat. This upper limit on capillary i.d., combined with the high separation efficiency and short observation times of CE, necessarily requires a detection method which can identify the presence of small amounts of material. As listed in Table 1, myriad techniques have been implemented as CE detectors.[120,121] Though these detection schemes generally exhibit good sensitivity, mass spectrometry is presently the only CE detector which yields rich chemical information about the analyte. Since NMR spectroscopy provides both confirmatory and complementary chemical information, it enables unprecedented levels of structural elucidation for CE detection. In addition, because of the ability of CE to concentrate analytes, samples with lower initial concentrations can utilize the enhanced S_m of improved NMR microprobes.

Although NMR can provide a wealth of unique structural information and CE has impressive separation capabilities, the coupling of CE with NMR detection has been demonstrated only recently.[58,79,80,88−92] Among the various separation techniques, CE is particularly amenable to solenoidal NMR microcells because the transceiver coil can be wrapped directly around the same fused silica capillary used in the separation. Sampling may occur via electrokinetic, gravimetric, or pressure injection. As such, NMR detection requires minimal modification of most existing CE equipment. In general, two different CE−NMR configurations have been demonstrated. In one arrangement,[58,79,80,91] both the inlet and outlet vials are housed within the NMR probe head (see Figure 13A). Presently, this setup requires that sample injection occur externally, followed by insertion into the magnet bore. In the other reported CE−NMR configuration,[88−92] the inlet vial remains outside of the magnet so that the probe remains stationary within the magnet during sample injection and separation (see Figure 13B). Future improvements will include the development of CE−NMR systems which allow automated injection, separation, and detection completely within the magnet.

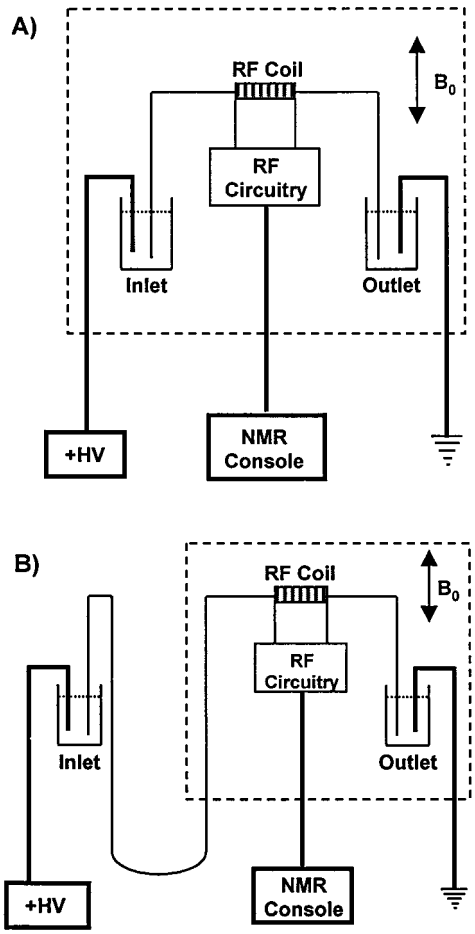

Figure 13. Configurations for electroseparations coupled with NMR detection: (A) both high-voltage inlet and grounded outlet within magnet bore, (B) inlet outside of magnet bore.

Despite relatively simple instrumental requirements, CE−NMR data reflects a complex interdependence on flow rate, electric field, and current. For instance, the current which passes through the capillary produces a magnetic field gradient that may perturb the uniformity of the B_0 field if it cannot be counteracted through shimming. For a cylindrical conductor which carries current i uniformly distributed over the cross-sectional area of the wire, Ampere's Law yields

$$B_I = \frac{\mu_0 i r}{2\pi R^2} \tag{8}$$

where B_I represents the current-induced magnetic field within the cylinder, μ_0 is the permeability constant, r is the radial distance from the center of the capillary, and R corresponds to the capillary inner diameter.[122] Because slight temperature variations within the capillary lead to minor changes in buffer conductivity, the current may not be exactly uniformly distributed across the cross-sectional area of the capillary. Nevertheless, this radial gradient varies linearly in magnitude to the extent that the current has a component in the B_0 direction. As shown in Figure 14, electrophoretic currents can

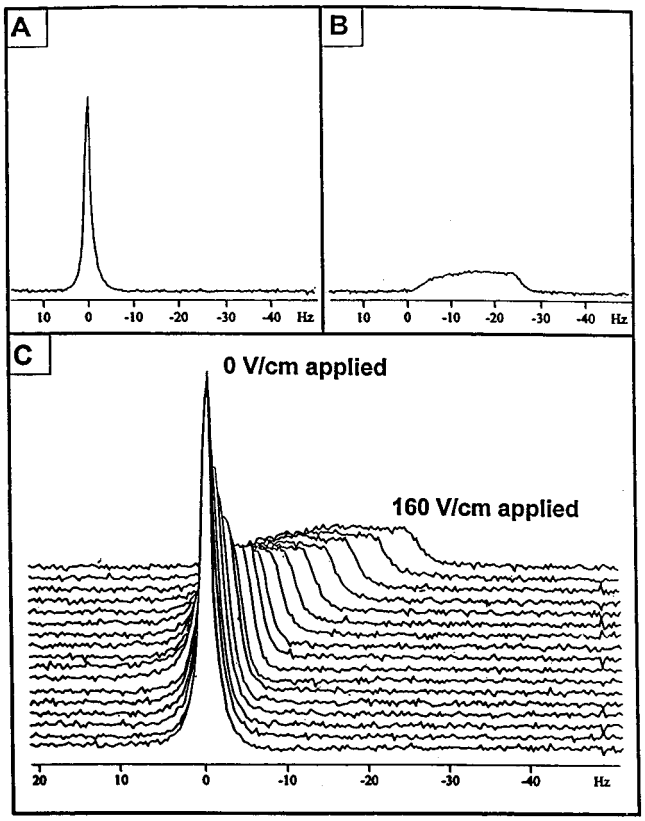

Figure 14. Signal degradation due to electrophoretic current: NMR signal from water in 50 mM sodium borate buffer (pH 9.3; 10% H_2O/90% D_2O). (A) Resonance signal referenced to 0 Hz with no applied voltage; S/N = 147; LW = 1.5 Hz. (B) Observed broadening and shift in resonance frequency with 8 kV applied over a 50 cm length of capillary; S/N =19; LW ≈ 19 Hz; i = 94 μA. (C) Series of spectra ranging from 0 to 160 V/cm in 10 V/cm increments. (Adapted with permission from ref 91. Copyright 1999 American Chemical Society.)

cause significant NMR signal degradation for a capillary configuration which is not parallel to B_0.[91] In addition to NMR spectral broadening due to current-induced magnetic field gradients, the high electric fields applied in capillary electroseparation techniques can partially align large molecules, thereby broadening signals. Although field strengths of ~90 V/cm have been shown to have a negligible effect on the LW of ^{1}H NMR spectra of amino acids,[88] the effects of higher electric field strengths on larger molecules has not been explored within the context of CE−NMR.

Investigations which compare pressure-driven and electroosmotic flow can isolate the effects of flow versus electrophoretic migration. In contrast to flowing HPLC−NMR experiments, CE has the characteristic that each separated analyte migrates at a different velocity and, therefore, has a different detector residence time.[123] For example, an electropherogram with peaks at 3 and 30 min exhibits detector residence times which differ by an order of magnitude. Therefore, a strategy of variable data acquisition time may be most suitable for optimizing S/N in on-line electrophoretic-NMR. For instance, limited observation time may be improved by decreasing or discontinuing the voltage to reduce or stop flow as the analyte enters the V_{obs} region. In this way,

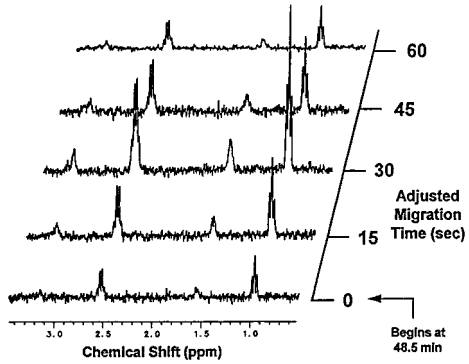

Figure 15. Periodic stopped-flow CE−NMR spectra illustrating sample stacking for a mixture of arginine (Arg) and triethylamine (TEA), both initially 50 mM. Each NMR spectrum is acquired with 40 co-added scans in 1 min, and a voltage of 7.0 kV is applied for 15 s between NMR data collections. TEA and Arg are concentrated by factors of 4.3 and 2.3, respectively. The first 48.5 min of migration time has been omitted for clarity. (Adapted with permission from ref 91. Copyright 1999 American Chemical Society.)

longer observation times can be applied to faster migrating analytes so that either a greater number of scans or a longer relaxation time between each scan can be used to enhance S/N. To eliminate both flow-induced and current-induced distortions of line width and shape, a unique stopped-flow strategy has been demonstrated where the CE voltage is periodically halted so that NMR information is obtained only under quiescent conditions.[91] This method of data acquisition cancels the effect of magnetic field gradients, increases the NMR S/N (due to longer observation times), and allows separation efficiencies on the order of 50 000. Additionally, preconcentration (stacking) methods[124] extend the usable sample concentration range of the method but do not generally affect NMR mass LODs. Figure 15 demonstrates the enhanced S/N which results when stacking conditions are utilized and illustrates the capability of NMR to monitor the concentration event directly and obtain spectra from lower concentrations of analytes.[91] While these initial concentration factors of 2−5-fold are rather modest compared to other reports of sample stacking in CE,[124,125] these results[91] represent the first examples of stacking to improve CE−NMR detectability. Clearly, future experiments will further extend the concentration range of suitable samples for CE−NMR.

While initial reports[79,80] of CE−NMR demonstrated the potential of coupling the high separation efficiency of CE with the capacity of structural analysis provided by NMR, original spectral LWs were larger than 7 Hz. Broad LWs make characterization of unknowns difficult, and the ~100 mM LODs precluded most assays. Subsequent improvements in microcoil NMR probe design[38,70,91] have resulted in high-resolution spectra and improved LODs. In addition to the solenoidal microcoil transceivers, saddle-type coils have recently been employed for CE−NMR.[88−90,92] More specifically, the 240-nL NMR detection cell described earlier has been utilized in conjunction with a 60-μm i.d. separation capillary for CE−NMR. With this arrangement, a separation of lysine and histidine was achieved with an esti-

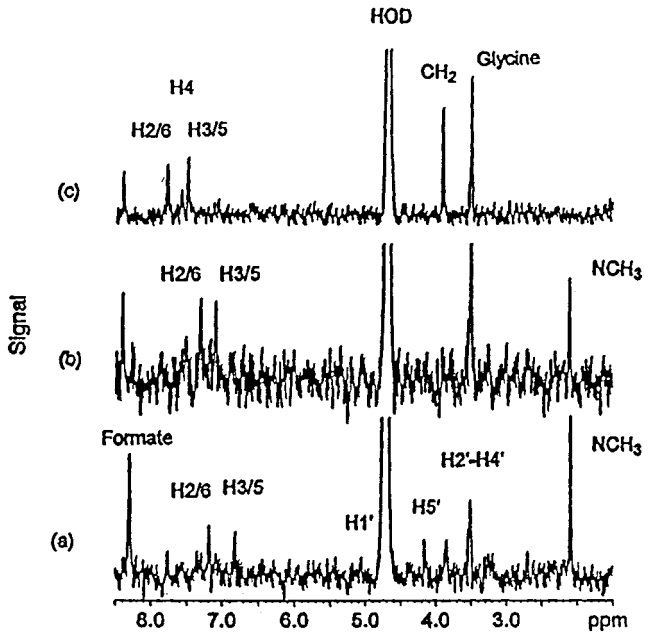

Figure 16. Single rows extracted from the CZE−NMR electropherogram of paracetamol metabolites: (A) paracetamol glucuronide, (B) paracetamol sulfate, (C) the endogenous material hippurate. (Adapted with permission from ref 90. Copyright 1998 Royal Society of Chemistry.)

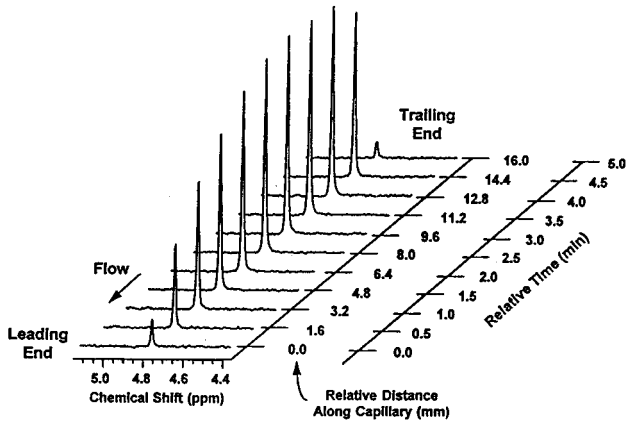

Figure 17. Monitoring CE injection profiles via observation of an H_2O plug through a microcoil NMR detector: The plug is gravimetrically injected, followed by application of a 7.0 kV potential across a 50-cm long capillary. Once the first H_2O peak is observed, the voltage is reduced to 0.7 kV. Single-scan spectra show the H_2O concentration increasing parabolically, followed by an abrupt trailing end. The relative time begins at an offset of 22 min, omitted for clarity. The relative position along the capillary is computed from the migration time and velocity to provide an indication of the total plug length as it reaches the microcoil detector. (Adapted with permission from ref 91. Copyright 1999 American Chemical Society.)

mated LOD_c of ~2 mM for lysine.[88] On the basis of the aliphatic and aromatic NMR signals, the amino acids could be distinguished. In two other reports of CE−NMR with saddle-type coils,[89,90] separation and detection of the major metabolic products of the analgesic drug paracetamol was demonstrated from an extract of human urine. Because the metabolism of paracetamol is well established and has been studied extensively with NMR spectroscopy,[126,127] this analyte and its metabolic products provide an attractive biological model system to evaluate the performance of capillary electroseparation systems coupled to NMR microprobes. Though an 8-nL injection volume was used for these CE−NMR experiments, a larger 400-nL NMR detection cell was created from an 80-μm i.d. capillary. As illustrated in Figure 16, the glucuronide and sulfate conjugates of the drug as well as a major endogenous species were identified from the ^{1}H NMR spectra of the electropherogram.[90] LODs for each of the analytes were estimated to be ~10 ng, but no indication of separation efficiency was given.

Since the electrophoretic current in the capillary is parallel to B_0 for saddle-type coils, the current-induced magnetic field and its deleterious effects on the NMR signals is minimized. On the other hand, the relatively large detector zones used in conjunction with these coils introduce significant band broadening and thus limit separation efficiency. With advances in the sensitivity of NMR probes and a better understanding of the challenges involved in coupling CE and NMR, this hyphenated technique is becoming practical in situations which require separation and structural determination of mass-limited unknowns.

In addition to structural identification of separated analytes, CE−NMR provides many unique opportunities to study fundamental electrophoretic phenomena in a nondestructive manner. Though not yet performed for capillaries, demonstrated capabilities of electrophoretic-NMR include direct measurement of pH,[128] selective detection of charged species,[129] diffusion coefficients,[130] mobilities,[129,130] and flow imaging.[131] As one example of the diagnostic information which is available in CE−NMR data, electroosmotic flow and solvent composition can be monitored directly. For an injection plug of 10% H_2O in D_2O, Figure 17 shows a leading parabolic-type concentration profile (originating from a gravimetric injection) and a trailing flat profile (caused by the application of an electrical potential after the injection). The length of the plug is consistent with contributions from injection and diffusion and indicates that other sources of zone spreading such as mixing are not significant.[91]

Other preliminary experiments have established an essentially linear relationship between LW and electroosmotic flow rate. In this fashion, LW can be used to measure the electroosmotic flow rate of a solvent and the electrophoretic migration rate of a charged species. By examining the LW, one can compute the coil residence time of the analyte and hence flow rates for all components in a CE separation as they migrate through the detector. Such information is difficult to obtain with other detection methods without perturbing the separation. This aspect of NMR detection in CE certainly has not yet been fully explored. A greater understanding of the fundamental separation mechanisms among the many CE modes of operation would aid in the development of improved or novel approaches.

E. CEC–NMR

As a hybrid of CE and HPLC, capillary electrochromatography has found increasing utility within

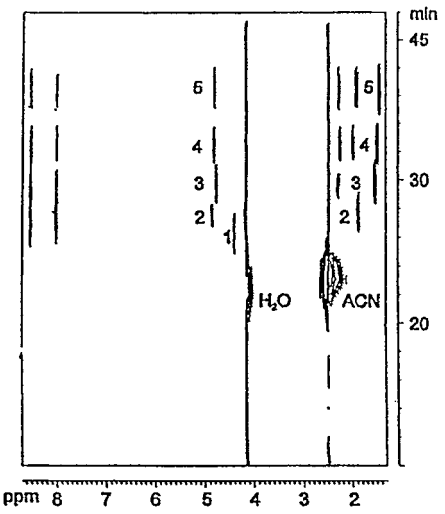

Figure 18. Contour plot of a CEC−NMR separation of five alkyl benzoates. (Adapted with permission from ref 88. Copyright 1998 American Chemical Society.)

the past decade.[132−134] With high electrical potentials applied across packed capillary columns, CEC features the selectivity of a stationary phase and eliminates the parabolic flow profile of pressure-driven separations. As a result, CEC has enjoyed significant success in the separation of a variety of charged and neutral species with high efficiencies.[135−137] Presently, only four reports of CEC−NMR have appeared in the literature.[88−90,92] In one of these examples, the 240-nL NMR detection capillary described previously was attached in series with a 20-cm length of 250-μm i.d. capillary packed with 5-μm particles.[88] The total capillary length was 220 cm with 110 cm from inlet to detector. As shown in Figure 18, five alkyl benzoates were separated and identified on-line with ^{1}H NMR detection.[88] Compared to a separation of the same five alkyl benzoates by capillary HPLC−NMR, the combination of pressure assistance and electroosmotic flow reduced the elution time in CEC−NMR by a factor of 2. Additionally, the improved chromatographic resolution of CEC−NMR (with respect to capillary HPLC−NMR) was attributed to the plug flow profile of electroosmosis. In stopped-flow mode, a two-dimensional ^{1}H−^{1}H COSY spectrum was acquired for pentyl benzoate to verify the coupling pattern of the monosubstituted aromatic hydrocarbon. Though not reported for CEC−NMR, LODs can be estimated in the hundreds of picomoles based upon the performance of the probe for a detection cell filled with analyte.

In two other accounts,[89,90] CEC−NMR was applied to the separation of metabolites of paracetamol. Optimal separation conditions were first established by conventional CEC with UV absorbance detection. For these CEC−NMR experiments, a 400-nL NMR detection cell was used and connected to a 250-μm i.d. capillary packed with 20 cm of stationary phase. While the observe volume was increased from the 240 nL used in the other CEC−NMR example,[88] f_c remains below 2% for this configuration. Because of the relatively low electric field used (<100 V/cm) and the long distance from inlet to detector, the separation required almost 1 h to complete. Nevertheless, on-line CEC−NMR data acquisition allowed the ^{1}H NMR detection and identification of the two major metabolites (i.e., the glucuronide and sulfate conjugates of the drug) as well as the endogenous material hippurate from an injection volume of 500 nL. In addition, a two-dimensional TOCSY experiment was performed overnight in stopped-flow CEC−NMR mode to provide confirmatory evidence of the glucuronide paracetamol conjugate. Given the metabolite concentration in urine and the observed NMR S/N, it was estimated that amounts in the low nanogram range were detected for each metabolite. Although the benefits of greater loading capacity and consequently improved NMR S/N for CEC compared to CE are evident, the authors make note of the technical difficulty of coupling capillary electroseparations and NMR detection. Despite these challenges, CEC−NMR offers the combination of highly efficient separations, increased sample loading capacity compared to CZE, and information-rich detection. As a result, this hyphenated technique will find extensive use in the future.

VIII. Conclusions

As techniques for chemical analysis are used in continually smaller domains, experimental challenges for inherently insensitive methods such as NMR become increasingly severe. Among the various schemes to increase the intrinsic sensitivity of an NMR experiment, the development of small-volume RF probes has experienced a renaissance during the past decade. Commercial NMR probes now allow analyses of nanomole quantities in microliter volumes from natural product extracts and combinatorial chemical syntheses. Although the development of nanoliter-volume probes is still in the research phase, the enhancements in sensitivity which have resulted from submillimeter-diameter coils are exciting. Through the fabrication of nanoliter-volume NMR probes and their coupling to microseparation strategies, mass-limited analytes in complex matrixes are becoming viable samples for NMR analysis. Recent demonstrations of on-line HPLC−NMR−MS have combined one of the most widely used separation methods with two of the most information-rich techniques of chemical characterization.[138−141] The extension of this doubly hyphenated method to the capillary scale will enable rapid, chemically rich screening of mass-limited samples with enhanced mass sensitivity.

While the increased sensitivity of reduced-diameter RF probes provides a widely applicable benefit for NMR spectroscopy, microcoils offer several additional advantages which have not been fully explored. As one example, the diminutive spatial dimensions of microcoil probes enable their use in low-homogeneity high-field magnets. One study reported increased spectral resolution from a series of microcoils with decreasing diameters within a magnet of poor (100 ppm/cm) homogeneity.[142] This property of microcoils enables their potential use as part of benchtop high-resolution NMR spectrometers.[143] Additionally, since the self-resonance frequency of microcoils lies in the GHz range,[57] their use within very high-field (i.e.,

>30 T) magnets is possible. Microcoils can also be applied to solid-state NMR. The short pulse widths of these coils are beneficial for wide-line spectroscopy and multipulse line-narrowing techniques. Since a rudimentary capillary spinner has been developed for high-resolution microcoil studies,[41] microcoil NMR can be expanded to include magic angle spinning of solid or semisolid samples. The reduced dimensions of the rotor would allow higher spin rates and thus yield more effective proton dipolar decoupling. Finally, the use of reduced-diameter RF probes for microimaging and NMR spectroscopic characterization of cellular samples has only begun to receive attention. Numerous areas in the biological sciences will undoubtedly benefit from improved NMR spectroscopy of small volumes in the coming decade.

IX. Acknowledgments

It is a pleasure to acknowledge Wayne Kelley and Andrew Wolters for their suggestions and helpful discussions in the preparation of this manuscript. We acknowledge support from the National Institutes of Health (GM53030) and the Camille and Henry Dreyfus Foundation (J.V.S.). M.E.L. appreciates the financial support of an NSF Graduate Fellowship. A.G.W. acknowledges the National Science Foundation for the support of a CAREER award (DBI 97-22320).

X. References

(1) Salzmann, M.; Pervushin, K.; Wider, G.; Senn, H.; Wüthrich, K. *Proc. Natl. Acad. Sci.* **1998**, *95*, 13585−90.
(2) Shapiro, M. J.; Wareing, J. R. *Curr. Opin. Chem. Biol.* **1998**, *2*, 372−5.
(3) Derome, A. E. *Modern NMR Techniques for Chemistry Research*; Pergamon Press Ltd.: New York, 1987.
(4) Ernst, R. R.; Bodenhausen, G.; Wokaun, A. *Principles of Nuclear Magnetic Resonance in One and Two Dimensions*; Oxford University Press: Oxford, 1991.
(5) Braun, S.; Kalinowski, H.-O.; Berger, S. *100 and More Basic NMR Experiments: A Practical Course*; VCH Publishers: New York, 1996.
(6) Günther, H. *NMR Spectroscopy: Basic Principles, Concepts, and Applications in Chemistry*; John Wiley & Sons Ltd.: Chichester, England, 1996.
(7) Hoult, D. I.; Richards, R. E. *J. Magn. Reson.* **1976**, *24*, 71−85.
(8) Long, H. W.; Gaede, H. C.; Shore, J.; Raven, L.; Bowers, C. R.; Kitzenberger, J.; Pietrass, T.; Pines, A. *J. Am. Chem. Soc.* **1993**, *115*, 8491−2.
(9) Navon, G.; Song, Y. Q.; Room, T.; Appelt, S.; Taylor, R. E.; Pines, A. *Science* **1996**, *271*, 1848−51.
(10) Fitzgerald, R. J.; Sauer, K. L.; Happer, W. *Chem. Phys. Lett.* **1998**, *284*, 87−92.
(11) Black, R. D.; Early, T. A.; Roemer, P. B.; Mueller, O. M.; Morgo-Campero, A.; Turner, L. G.; Johnson, G. A. *Science* **1993**, *259*, 793−5.
(12) Hill, H. D. *Appl. Supercond.* **1997**, *7*, 3750−5.
(13) Marek, D.; Haeberli, M.; Triebe, R.; Warden, M.; Baselgia, L.; Gerfin, T.; Schett, O.; Laukien, F. *Ultra Sensitive High-Resolution NMR Probes*; Experimental NMR Conference, Orlando, FL, 1997, Poster 122.
(14) Pease, J.; Withers, R.; Nast, R.; Deese, A.; Calderon, P.; Mehta, S.; Kelly, T.; Laukien, F. *Application of a 2.5-mm CryoProbe to Metabolite Studies*; Experimental NMR Conference, Orlando, FL, 1999, Poster 202.
(15) Müller-Warmuth, W.; Meise-Gresch, K. *Adv. Magn. Reson.* **1983**, *11*, 1.
(16) Dorn, H. C.; Gu, J.; Bethune, D. S.; Johnson, R. D.; Yannoni, C. S. *Chem. Phys. Lett.* **1993**, *203*, 549−54.
(17) Gitti, R.; Wild, C.; Tsiao, C.; Zimmer, K.; Glass, T. E.; Dorn, H. C. *J. Am. Chem. Soc.* **1988**, *110*, 2294−6.
(18) Stevenson, S.; Dorn, H. C. *Anal. Chem.* **1994**, *66*, 2993−9.
(19) Stevenson, S.; Glass, T.; Dorn, H. C. *Anal. Chem.* **1998**, *70*, 2623−8.
(20) Odelblad, E. Micro-NMR in High Permanent Magnetic Fields. *Nordisk Forening for Obsterik och Gynekologi*; Karolinska Institute: Stockholm, 1966.
(21) Shoolery, J. N. *Top. Carbon-13 NMR Spectrosc.* **1979**, *3*, 28−38.
(22) Wiseman, R. W.; Moerland, T. S.; Kushmerick, M. J. *NMR Biomed.* **1993**, *6*, 153−6.
(23) Cho, Z.; Ahn, C.; Juh, S.; Lee, H. *Med. Phys.* **1988**, *15*, 815−24.
(24) Glover, P. M.; Bowtell, R. W.; Brown, G. D.; Mansfield, P. *Magn. Reson. Med.* **1994**, *31*, 423−8.
(25) Hsu, E. W.; Aiken, N. R.; Blackband, S. J. *Am. J. Physiol.—Cell Physiol.* **1996**, *40*, C1895−C1900.
(26) Hsu, E. W.; Aiken, N. R.; Blackband, S. J. *Magn. Reson. Med.* **1997**, *37*, 624−7.
(27) Aiken, N. R.; Hsu, E. W.; Horsman, A.; Blackband, S. J. *Am. J. Physiol.—Cell Physiol.* **1996**, *40*, C1295−C1302.
(28) Schoeniger, J. S.; Aiken, N.; Hsu, E.; Blackband, S. J. *J. Magn. Reson. Ser. B* **1994**, *103*, 261−73.
(29) Sanny, J.; Clark, W. G. *Rev. Sci. Instrum.* **1981**, *52*, 539−41.
(30) Mahdjour, J.; Clark, W. G.; Baberschke, K. *Rev. Sci. Instrum.* **1986**, *57*, 1100−6.
(31) Ohno, K.; Murakami, T. *J. Magn. Reson.* **1988**, *79*, 343−7.
(32) Maple, S. R.; Allerhand, A. *J. Magn. Reson.* **1986**, *66*, 168−71.
(33) Hoch, J. C.; Stern, A. S. *NMR Data Processing*; Wiley-Liss, Inc.: New York, 1996.
(34) Fuks, L. F.; Huang, F. S. C.; Carter, C. M.; Edelstein, W. A.; Roemer, P. B. *J. Magn. Reson.* **1992**, *100*, 229−42.
(35) VanderHart, D. L. Magnetic Susceptibility & High-Resolution NMR of Liquids & Solids. In *Encyclopedia of Nuclear Magnetic Resonance*; Grant, D. M., Harris, R. K., Eds.; John Wiley & Sons: New York, 1996; Vol. 5, pp 2938−46.
(36) Doty, F. D.; Entzminger, G.; Yang, Y. A. *Conc. Magn. Reson.* **1998**, *10*, 133−56.
(37) ASTM E 386-90. *Annu. Book ASTM Stand.* **1997**, *3.06*, 731−9.
(38) Olson, D. L.; Peck, T. L.; Webb, A. G.; Magin, R. L.; Sweedler, J. V. *Science* **1995**, *270*, 1967−70.
(39) Reynolds, W. F.; Yu, M.; Enriquez, R. G. *Magn. Reson. Chem.* **1997**, *35*, 614−8.
(40) Wilmad Glass Product Catalog. http://www.wilmad.com (accessed May 1999).
(41) Behnia, B.; Webb, A. G. *Anal. Chem.* **1998**, *70*, 5326−31.
(42) Shoolery, J. N. *Varian Instrum. Appl.* **1976**, *10*, 18−9.
(43) Shoolery, J. N.; Wehrli, F.; Wirthlin, T. *Chem.-Technol. (Heidelberg)* **1977**, *6*, 55−9.
(44) Shoolery, J. N.; Majors, R. E. *Am. Lab.* **1977**, *9*, 51−61.
(45) Chatterjee, A.; Mukhopadhyay, S.; Shoolery, J. N. *Indian J. Chem.* **1978**, *16B*, 67−8.
(46) Shoolery, J. N.; Southwick, E. W. *J. Agric. Food Chem.* **1979**, *27*, 1400−2.
(47) Crouch, R. C.; Martin, G. E. *Magn. Reson. Chem.* **1992**, *30*, S66−S70.
(48) Shockcor, J. P.; Wurm, R. M.; Silver, I. S.; Crouch, R. C.; Martin, G. E. *Tetrahedron Lett.* **1994**, *35*, 4919−22.
(49) Crouch, R. C.; Martin, G. E. *J. Nat. Prod.* **1992**, *55*, 1343−7.
(50) Crouch, R. C.; Martin, G. E.; Musser, S. M.; Grenade, H. R.; Dickey, R. W. *Tetrahedron Lett.* **1995**, *36*, 6827−30.
(51) Sharaf, M. H. M.; Schiff, P. L., Jr.; Tackie, A. N.; Phoebe, C. H., Jr.; Howard, L.; Meyers, C.; Hadden, C. E.; Wrenn, S. K.; Davis, A. O.; Andrews, C. W.; Minick, D.; Johnson, R. L.; Shockcor, J. P.; Crouch, R. C.; Martin, G. E. *Magn. Reson. Chem.* **1995**, *33*, 767−78.
(52) Martin, G. E.; Crouch, R. C.; Zens, A. P. *Magn. Reson. Chem.* **1998**, *36*, 551−7.
(53) Martin, G. E.; Guido, J. E.; Robins, R. H.; Sharaf, M. H. M.; Schiff, P. L.; Tackie, A. N. *J. Nat. Prod.* **1998**, *61*, 555−9.
(54) Hadden, C. E.; Martin, G. E. *J. Nat. Prod.* **1998**, *61*, 969−72.
(55) Barbara, T. M. *J. Magn. Reson. A* **1994**, *109*, 265−9.
(56) Peck, T. L.; Magin, R. L.; Lauterbur, P. C. *J. Magn. Reson. B.* **1995**, *108*, 114−24.
(57) Webb, A. G. *Prog. Nucl. Magn. Reson. Spectrosc.* **1997**, *31*, 1−42.
(58) Olson, D. L.; Lacey, M. E.; Sweedler, J. V. *Anal. Chem.* **1998**, *70*, 257A−64A.
(59) Rao, N. N. *Electromagnetics*; Prentice Hall: New York, 1992.
(60) Muller, L. *J. Am. Chem. Soc.* **1979**, *101*, 4481−4.
(61) Bax, A.; Griffey, R. H.; Hawkins, B. L. *J. Magn. Reson.* **1983**, *55*, 301−15.
(62) Bodenhausen, G.; Ruben, D. J. *Chem. Phys. Lett.* **1980**, *6*, 185−9.
(63) Kay, L. E.; Ikura, M.; Tschudin, R.; Bax, A. *J. Magn. Reson.* **1990**, *89*, 496−514.
(64) Grzesiek, S.; Bax, A. *J. Magn. Reson.* **1992**, *96*, 432−40.
(65) Rogers, J. A.; Jackman, R. J.; Whitesides, G. M.; Olson, D. L.; Sweedler, J. V. *Appl. Phys. Lett.* **1997**, *70*, 2464−6.
(66) Peck, T. L.; Magin, R. L.; Kruse, J.; Feng, M. *IEEE Trans. Biomed. Eng.* **1994**, *41*, 706−9.
(67) Stocker, J. E.; Peck, T. L.; Webb, A. G.; Feng, M.; Magin, R. L. *IEEE Trans. Biomed. Eng.* **1997**, *44*, 1122−7.
(68) Trumbull, J. D.; Glasgow, I. K.; Beebe, D. J.; Magin, R. L. *IEEE Trans. Biomed. Eng.*, in press.

(69) Webb, A. G.; Grant, S. C. *J. Magn. Reson. B* **1996**, *113*, 83−7.
(70) Olson, D. L.; Lacey, M. E.; Sweedler, J. V. *Anal. Chem.* **1998**, *70*, 645−50.
(71) Chauret, D. C.; Durst, T.; Arnason, J. T.; Sanchez-Vindas, P.; Roman, L. S.; Poveda, L.; Keifer, P. A. *Tetrahedron Lett.* **1996**, *37*, 7875−8.
(72) Manzi, A.; Salimath, P. V.; Spiros, R. C.; Keifer, P. A.; Freeze, H. H. *J. Biol. Chem.* **1995**, *270*, 9154−63.
(73) Delepierre, M.; Roux, P.; Chaffotte, A. F.; Goldberg, M. E. *Magn. Reson. Chem.* **1998**, *36*, 645−50.
(74) Delepierre, M.; Prochnicka-Chalufour, A.; Possani, L. D. *Biochemistry* **1997**, *36*, 2649−58.
(75) Fitch, W. L.; Detre, G.; Holmes, C. P.; Shoolery, J. N.; Keifer, P. A. *J. Org. Chem.* **1994**, *59*, 7955−6.
(76) Keifer, P. A.; Baltusis, L.; Rice, D. M.; Tymiak, A. A.; Shoolery, J. N. *J. Magn. Reson. A* **1996**, *119*, 65−75.
(77) Garigipati, R. S.; Adams, B.; Adams, J. L.; Sarkar, S. K. *J. Org. Chem.* **1996**, *61*, 2911−4.
(78) Sarkar, S. K.; Garigipati, R. S.; Adams, J. L.; Keifer, P. A. *J. Am. Chem. Soc.* **1996**, *118*, 2305−6.
(79) Wu, N.; Peck, T. L.; Webb, A. G.; Magin, R. L.; Sweedler, J. V. *J. Am. Chem. Soc.* **1994**, *116*, 7929−30.
(80) Wu, N.; Peck, T. L.; Webb, A. G.; Magin, R. L.; Sweedler, J. V. *Anal. Chem.* **1994**, *66*, 3849−57.
(81) Wu, N.; Webb, A.; Peck, T. L.; Sweedler, J. V. *Anal. Chem.* **1995**, *67*, 3101−7.
(82) Subramanian, R.; Lam, M. M.; Webb, A. G. *J. Magn. Reson.* **1998**, *133*, 227−31.
(83) Subramanian, R.; Webb, A. G. *Anal. Chem.* **1998**, *70*, 2454−8.
(84) Subramanian, R.; Sweedler, J. V.; Webb, A. G. *J. Am. Chem. Soc.* **1999**, *121*, 2333−4.
(85) Korhammer, S. A.; Bernreuther, A. *Fresenius J. Anal. Chem.* **1996**, *354*, 131−5.
(86) Albert, K. *J. Chromatogr. A* **1997**, *785*, 65−83.
(87) Albert, K. *J. Chromatogr.* **1995**, *703*, 123−47.
(88) Pusecker, K.; Schewitz, J.; Gfrörer, P.; Tseng, L.-H.; Albert, K.; Bayer, E. *Anal. Chem.* **1998**, *70*, 3280−5.
(89) Pusecker, K.; Schewitz, J.; Gfrörer, P.; Tseng, L.-H.; Albert, K.; Bayer, E.; Wilson, I. D.; Bailey, N. J.; Scarfe, G. B.; Nicholson, J. K.; Lindon, J. C. *Anal. Commun.* **1998**, *35*, 213−5.
(90) Schewitz, J.; Gfrörer, P.; Pusecker, K.; Tseng, L.-H.; Albert, K.; Bayer, E.; Wilson, I. D.; Bailey, N. J.; Scarfe, G. B.; Nicholson, J. K.; Lindon, J. C. *Analyst* **1998**, *123*, 2835−7.
(91) Olson, D. L.; Lacey, M. E.; Webb, A. G.; Sweedler, J. V. *Anal. Chem.* **1999**, *71*, 3070−6.
(92) Gfrörer, P.; Schewitz, J.; Pusecker, K.; Tseng, L.-H.; Albert, K.; Bayer, E. *Electrophoresis* **1999**, *20*, 3−8.
(93) Lindon, J. C.; Nicholson, J. K.; Wilson, I. D. *Prog. Nucl. Magn. Reson. Spectrosc.* **1996**, *29*, 1−49.
(94) Albert, K.; Dachtler, M.; Glaser, T.; Händel, H.; Lacker, T.; Schlotterbeck, G.; Strohschein, S.; Tseng, L.-H.; Braumann, U. *J. High Resolut. Chromatogr.* **1999**, *22*, 135−43.
(95) Laude, D. A., Jr.; Wilkins, C. L. *Anal. Chem.* **1984**, *56*, 2471−5.
(96) Dorn, H. C. *Anal. Chem.* **1984**, *56*, 747A−58A.
(97) Tallarek, U.; Bayer, E.; Guiochon, G. *J. Am. Chem. Soc.* **1998**, *120*, 1494−505.
(98) Watanabe, N.; Niki, E. *Proc. Jpn. Acad., Ser. B* **1978**, *54*, 194−9.
(99) Bayer, E.; Albert, K.; Nieder, M.; Grom, E.; Keller, T. *J. Chromatogr.* **1979**, *186*, 497−507.
(100) Curran, S. A.; Williams, D. E. *Appl. Spectrosc.* **1987**, *41*, 1450−4.
(101) Glass, T. E.; Dorn, H. C. *J. Magn. Reson.* **1983**, *51*, 527−30.
(102) Haw, J. F.; Glass, T. E.; Dorn, H. C. *J. Magn. Reson.* **1982**, *49*, 22−31.
(103) Griffiths, L. *Magn. Reson. Chem.* **1997**, *35*, 257−61.
(104) Griffiths, L. *Anal. Chem.* **1995**, *67*, 4091−5.
(105) Sudmeier, J. L.; Günther, U. L.; Albert, K.; Bachovchin, W. W. *J. Magn. Reson., Ser. A* **1996**, *118*, 145−56.
(106) Bayer, E.; Albert, K.; Nieder, M.; Grom, E.; Wolff, G.; Rindlisbacher, M. *Anal. Chem.* **1982**, *54*, 1747−50.
(107) Sidelmann, U. G.; Gavaghan, C.; Carless, H. A. J.; Spraul, M.; Hofmann, M.; Lindon, J. C.; Wilson, I. D.; Nicholson, J. K. *Anal. Chem.* **1995**, *67*, 4441−5.
(108) Laude, D. A., Jr.; Lee, R. W.-K.; Wilkins, C. L. *Anal. Chem.* **1985**, *57*, 1464−9.
(109) Smallcombe, S. H.; Patt, S. L.; Keifer, P. A. *J. Magn. Reson.* **1995**, *117*, 295−303.
(110) Behnke, B.; Schlotterbeck, G.; Tallarek, U.; Strohschein, S.; Tseng, L.-H.; Keller, T.; Albert, K.; Bayer, E. *Anal. Chem.* **1996**, *68*, 1110−5.
(111) Albert, K.; Schlotterbeck, G.; Tseng, L.-H.; Braumann, U. *J. Chromatogr. A* **1996**, *750*, 303−9.
(112) Schlotterbeck, G.; Tseng, L.-H.; Händel, H.; Braumann, U.; Albert, K. *Anal. Chem.* **1997**, *69*, 1421−5.
(113) Albert, K.; Braumann, U.; Tseng, L.-H.; Nicholson, G.; Bayer, E.; Spraul, M.; Hofmann, M.; Dowle, C.; Chippendale, M. *Anal. Chem.* **1994**, *66*, 3042−6.
(114) Allen, L. A.; Glass, T. E.; Dorn, H. C. *Anal. Chem.* **1988**, *60*, 390−4.
(115) Albert, K.; Braumann, U.; Streck, R.; Spraul, M.; Ecker, R. *Fresenius' J. Anal. Chem.* **1995**, *352*, 521−8.
(116) Braumann, U.; Händel, H.; Albert, K.; Ecker, R.; Spraul, M. *Anal. Chem.* **1995**, *67*, 930−5.
(117) Braumann, U.; Händel, H.; Strohschein, S.; Spraul, M.; Krack, G.; Ecker, R.; Albert, K. *J. Chromatogr. A* **1997**, *761*, 336−40.
(118) *Handbook of Capillary Electrophoresis*; Landers, J. P., Ed.; CRC Press: Boca Raton, FL, 1994.
(119) Beale, S. C. *Anal. Chem.* **1998**, *70*, 279R−300R.
(120) Jorgenson, J. W.; De Wit, J. Detection in Microcolumn Liquid Chromatography. In *Detectors for Capillary Chromatography*; Hill, H. H., McMinn, D. G., Eds.; Chemical Analysis: A Series of Monographs on Analytical Chemistry and Its Applications 121; John Wiley & Sons: New York, 1992.
(121) Cruz, L. A.; Shippy, S. A.; Sweedler, J. V. Capillary Electrophoresis Detectors Based on Light. In *High Performance Capillary Electrophoresis*; Khaledi, M., Ed.; John Wiley & Sons: New York, 1998; pp 303−54.
(122) Ohanian, H. C. *Physics*, 2nd ed.; W. W. Norton & Co.: New York, 1989; pp 753−5.
(123) Huang, X.; Coleman, W. F.; Zare, R. N. *J. Chromatogr.* **1989**, *480*, 95−110.
(124) Burgi, D. S.; Chien, R. L. Application and Limits of Sample Stacking in Capillary Electrophoesis. In *Capillary Electrophoresis Guidebook: Principles, Operations, and Applications*, Altria, K. D., Ed.; Humana Press: Totowa, NJ, 1997; pp 211−26.
(125) Quirino, J. P.; Terabe, S. *Science* **1998**, *282*, 465−6.
(126) Bales, J. R.; Sadler, P. J.; Nicholson, J. K.; Timbrell, J. A. *Clin. Chem.* **1984**, *30*, 1631−36.
(127) Bales, J. R.; Nicholson, J. K.; Sadler, P. J. *Clin. Chem.* **1985**, *31*, 757−62.
(128) Lawrence, B. A.; Polse, J.; DePina, A.; Allen, M. M.; Kolodny, N. H. *Curr. Microbiol.* **1997**, *34*, 280−3.
(129) Heil, S. R.; Holz, M. *Angew. Chem., Int. Ed. Engl.* **1996**, *35*, 1717−20.
(130) Hinton, D. P.; Johnson, C. S. *J. Colloid Interface Sci.* **1995**, *173*, 364−71.
(131) Wu, D.; Chen, A.; Johnson, C. S. *J. Magn. Reson. A* **1995**, *115*, 123−6.
(132) Crego, A. L.; González, A.; Marina, M. L. *Crit. Rev. Anal. Chem.* **1996**, *26*, 261−304.
(133) Colón, L. A.; Guo, Y.; Fermier, A. *Anal. Chem.* **1997**, *70*, 4461A−67A.
(134) Robson, M. M.; Cikalo, M. G.; Myers, P.; Euerby, M. R.; Bartle, K. D. *J. Microcolumn Sep.* **1997**, *9*, 357−72.
(135) Smith, N. W.; Evans, M. B. *Chromatographia* **1994**, *38*, 649−57.
(136) Yan, C.; Rakestraw, D. J. *Anal. Chem.* **1995**, *67*, 2026−9.
(137) Tan, Z. J.; Remcho, V. T. *Electrophoresis* **1998**, *19*, 2055−60.
(138) Pullen, F. S.; Swanson, A. G.; Newman, M. J.; Richards, D. S. *Rapid Commun. Mass Spectrom.* **1995**, *9*, 1003−6.
(139) Shockcor, J. P.; Unger, S. E.; Wilson, I. D.; Foxall, P. J. D.; Nicholson, J. K.; Lindon, J. C. *Anal. Chem.* **1996**, *68*, 4431−5.
(140) Burton, K. I.; Everett, J. R.; Newman, M. J.; Pullen, F. S.; Richards, D. S.; Swanson, A. G. *J. Pharm. Biomed. Anal.* **1997**, *15*, 1903−12.
(141) Dear, G. J.; Ayrton, J.; Plumb, R.; Sweatman, B. C.; Ismail, I. M.; Fraser, I. J.; Mutch, P. J. *Rapid Commun. Mass Spectrom.* **1998**, *12*, 2023−30.
(142) Wright, A. C.; Neideen, T. A.; Magin, R. L.; Norcross, J. A. *Rev. Sci. Instrum.* **1998**, *69*, 3938−41.
(143) Magin, R. L.; Webb, A. G.; Peck, T. L. *IEEE Spectrum* **1997**, *34*, 51−61.

CR980140F